Davidson Laboratory

Marine Hydrodynamics,
Coastal & Ocean Engineering

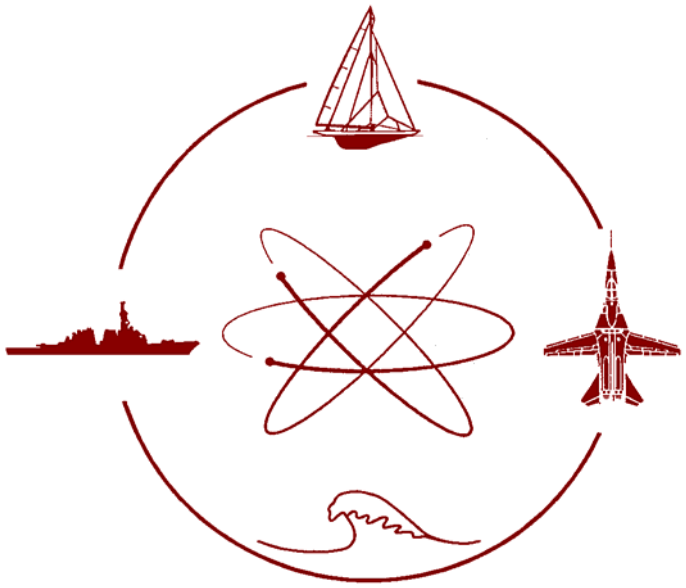

TECHNICAL REPORT SIT-DL-10-1-2882

January, 2010

Origin and Characteristics of the Spray Patterns Generated by Planing Hulls

by

Daniel Savitsky
Michael Morabito

STEVENS
Institute of Technology

Castle Point on Hudson,
Hoboken, NJ 07030

TR-2882

Davidson Laboratory
Stevens Institute of Technology
Hoboken, New Jersey 07030

ORIGIN AND CHARACTERISTICS OF THE SPRAY PATTERNS GENERATED BY PLANING HULLS

Report No 2882

By

Daniel Savitsky*
Michael Morabito**

January, 2010

---

* Professor Emeritus, Stevens Institute of Technology
** Research Engineer, Davidson Laboratory, Stevens Institute of Technology
Presented at the March 2010 meeting of the New York Metropolitan Section
of The Society of Naval Architects and Marine Engineers.

Origin and Characteristics of the Spray Patterns Generated by Planing Hulls

Author Names: *Daniel Savitsky,* ***Member***
Michael Morabito, ***Associate Member***

ABSTRACT

Analytical and experimental studies were made of the origin and characteristics of the two distinctly different appearing spray patterns associated with prismatic planing hulls. It was found that these two spray patterns, identified as "whisker spray" and "main spray", are a consequence of the same basic hydrodynamic flow phenomenon and transform seamlessly from one into the other.

Similar to the analytical treatment developed for swept-wing aircraft, where the oncoming free stream velocity is divided into components normal to and along the leading edge of the swept wing, the free stream velocity for the planing surface is divided into components normal to and along the stagnation line. Combining this orientation of velocity components with the results of analytical studies of H. Wagner (1932) for two-dimensional planing of infinitely long flat planing surfaces with those of A. E. Green (1935) for planing of a two dimensional, finite length surface, explains the origin and characteristics of both the whisker and main spray patterns. It is shown that the main spray originates in a small local area at the intersection of the stagnation line with the chine. Relatively simplistic equations, that define the three dimensional location of the spray apex, are developed and the results presented in three graphs. An illustrative example is presented that demonstrates the ease of application of the method to define the main spray geometry of a typical planing craft.

Model tests were conducted to define the maximum height of the main spray and its lateral and longitudinal positions relative to the hull as a function of deadrise angle, trim angle and speed coefficient. These data substantiate the analytical results.

KEY WORDS: planing hulls, main spray, whisker spray

NOMENCLATURE

b = chine beam (ft, m)
Cv = speed coefficient = $V/\sqrt{gb}$
l = length of flat plate (ft, m)
l_1 = distance from trailing edge to stagnation point of flat plate (ft, m)
l_2 = distance from stagnation point to leading edge of flat plate (ft, m)
lm = distance from trailing edge to spray root of flat plate (ft, m)
ls = length of stagnation line, between keel and chine (ft, m)
l_{WL} = static wetted length of flat plate (ft, m)
Lc = wetted chine length (beams)
Lk = wetted keel length (beams)
Ltr = length of spray trajectory from the intersection of the chine and the stagnation line to the point of maximum height in the horizontal plane (ft, m)
Lws = length of whisker spray along chine (ft, m)
V = speed of planing hull (ft/sec, m/sec)
Vn = velocity component normal to stagnation line (ft/sec, m/sec)
Vk = speed of planing hull (knots)
Vs = velocity component along stagnation line (ft/sec, m/sec)
Vv = vertical velocity of spray (ft/sec, m/sec)
tm = time to reach maximum height of trajectory (seconds)
X = horizontal distance between main spray origin and maximum height of main spray (ft, m)
Y = lateral distance between side of hull and maximum height of main spray (ft, m)

Z = maximum height of main spray relative to level water surface (ft, m)
X' = horizontal distance between main spray origin and maximum height of main spray (beams)
Y' = lateral distance between side of hull and maximum height of main spray (beams)
Z' = maximum height of main spray relative to level water surface (beams)

α = angle between stagnation line and keel, deg
β = deadrise angle, deg.
βe = effective angle of deadrise measured in a plane normal to the bottom and along the stagnation line, deg
βt = reduction of trajectory angle due to the geometric effect of trim angle, deg
γ = trajectory angle of main spray with respect to level water at chine, deg
Δ = displacement
θ = swept angle of wing, deg.
σ = spray thickness, in fractions of wetted length
τ = trim angle, deg
τ_{RAD} = trim angle, radians

INTRODUCTION

A typical spray formation associated with planing hulls is shown on Fig.1. Two distinct spray patterns are evident in this photograph. One is the so-called 'whisker" spray and the other is called the main spray. Characteristically, the whisker spray is a thin, light, spray consisting of droplets of water that are projected outboard of the chine at a trajectory angle essentially equal to the local hull deadrise angle. The main spray is a discharge of water in the form of a cone whose apex is in the vicinity of the stagnation line intersection with the chine and whose outboard trajectory is elevated significantly relative to that of the whisker spray. While distinctly different in appearance, this report demonstrates that both spray patterns are a consequence of the same hydrodynamic phenomenon.

Because of the large volume of water and the high trajectory angle of the main spray, it can impinge upon the wings and propellers of seaplanes to produce structural damage; it can also impact the tunnel between the hulls of a planing catamaran (with symmetric hulls) to significantly increase the hull resistance; and in a head wind it can be blown into the craft making for an uncomfortably wet environment. In addition, it may impact the wings of a "wing in ground effect" (WIG) craft since these marine vehicles require the wings to be located at relatively small distances above the water. A designer would be well served if the trajectory of the main spray was defined in terms of hull geometry and operating conditions.

Savitsky and Breslin (1958) conducted a series of tests of four constant deadrise hulls towed behind a wind screen to define the geometry of the main spray (prior to its breakup into intense droplets) as a function of hull deadrise angle, trim angle, and speed coefficient. The focus of that study was on the operating conditions of seaplanes and the distribution of the test results was limited to designers of seaplanes and to agencies of the United States government. Unfortunately, the small craft design community is generally unaware of the existence of this effort.

The present study develops an analytical method for defining the origin and geometry of the spray components and their locations relative to the planing hull. Also, a model test program was carried out to measure the spray geometry as a function of hull deadrise, trim angle and speed and to compare the results with the analytical predictions. In contrast to the test conditions of Savitsky and Breslin, (1958), where a wind screen was towed ahead of the model and measurements of the spray heights were made prior to the break-up of the spray into droplets, the present test program did not include a wind-screen and spray heights were measured from the level water surface to the top of the broken-spray

ORIGIN OF SPRAY PATTERNS DEVELOPED BY A PLANING HULL

Geometric Appearance of Hull Intersection with Free Water Surface

In order to describe the origin of the two basic spray forms associated with high speed planing hulls it is first necessary to describe the free water surface intersections with the hull as shown on the sketches in Fig. 2.

At pre-planing speeds the spray patterns do not develop but rather a small bow wave originates at the chine intersection with the water surface. This bow wave is a divergent wave formation and is akin to the gravity waves that exist for displacement vessels. At low speeds, the bow wave is the only visible water surface disturbance. As the speed increases, droplets of whisker spray and a small main spray blister appear slightly outboard of the crest of the bow wave. At high planing speeds the whisker and main spray formations become higher and larger so that they dominate

and completely obscure the bow wave. For all speeds, the height of bow wave crest is relatively small. These characteristics are demonstrated by a series of photographs taken by Savitsky and Breslin (1958). These are reproduced and discussed in the test section of this report.

While many of the notations in Fig. 2 are self explanatory, it is important to define the stagnation line and the spray root line. Specifically, the stagnation line is a locus of points on the bottom along which the flow is divided into forward and aft components and on which the pressure is a maximum and is developed from bringing to rest the component of free stream velocity normal to this line. (further discussion is given in a subsequent section of this report). Just forward of the stagnation line is the so-called spray root line. This defines the forward extent of the wetted bottom area when planing. According to theoretical (Wagner, 1932) and experimental (typically Savitsky and Neidinger, 1954) results, the actual wetted width at any cross section through the bottom is essentially $\pi/2$ times the wetted width defined by the level water line intersection with the bottom. This is referred to as the "wave-rise' factor. The angle of the spray root line, α, relative to the keel measured in a plane normal to the hull centerline and along the keel can be established from a knowledge of the deadrise, trim and $\pi/2$ wave rise factor. Thus, it can be shown that:

$$\alpha = Tan^{-1}\left(\frac{\pi}{2}\frac{\tan\tau}{\tan\beta}\right) \qquad \text{Eq. 1}$$

Because the stagnation line and the spray root line are very close to each other, the $\pi/2$ wave rise factor is often applied to both lines.

Also shown on Fig.2 is the forward extent of the whisker spray area. Subsequent sections of this paper compute the angle between the keel and the forward boundary of this spray component. Savitsky, Delorme, and Datla, (2007) presented a method for estimating the viscous resistance of the fluid that traverses this hull bottom area before being projected from the chines to become the visible whisker spray.

Fluid Flow Pattern along the Stagnation Line

To provide an understanding of the flow directions along the bottom of a planing hull, short lengths of soft fiber tufts were attached to the bottom of a prismatic deadrise hull. Fig.3 is an underwater photograph showing the alignment of the tufts with the hull underway. It is immediately apparent that the tufts are aligned with the stagnation line, thus indicating a velocity component that is directed along this line from keel to chine. Of further interest regarding this flow pattern are the results of bottom pressure measurements made by Smiley (1951). It was shown that, except at the chine where the pressure must be atmospheric, the pressure distribution along the stagnation line is constant (see Fig. 4). Thus, according to the Bernoulli equation, and excluding viscous effects, the velocity along this line is essential constant.

This is an important observation that confirms assumptions by other researchers (i.e. Pierson & Leshnover, 1950) that the resultant three-dimensional flow pattern in the chines-dry region of planing hulls can be decomposed into two components; one along the line and the other normal to the stagnation line. This is analogous to the aerodynamic treatment of flows over swept-back wings, where the free stream velocity, V, is resolved into components normal to, Vn, and along the span, Vs, of the wing leading edge as shown in Fig.5a. For the case of a planing surface the free stream velocity can be resolved into components normal to (Vn), and along the stagnation line (Vs) as shown in Fig.5b. As will be demonstrated in the subsequent sections of this report, this representation forms the foundation for describing the common origin of both the whisker spray and the main spray.

Using the equation for the angle α defined in Eq. 1:

$$Vn = V\sin\alpha \qquad \text{Eq. 2}$$

$$Vs = V\cos\alpha \qquad \text{Eq. 3}$$

The Spray Patterns in Two-Dimensional Planes

Since Vs is essentially constant along the stagnation line, it follows that the flow in planes normal to the stagnation line (Vn) may be treated as two-dimensional flows. Fig. 6 is sketch of the chines dry region of a planing hull. Considering planes normal to the stagnation line (sections k-c), it can be assumed that the fluid flow in these sections is equivalent to the flow about an equivalent flat plate planing at an effective trim angle τ' and a velocity Vn. If the plane k-c is taken fixed in space and the planing surface is made to pass through this plane at constant V, an examination of the changing

flow patterns in plane k-c will lead to a possible physical explanation for the origin of both the whisker and main sprays.

Consider consecutive positions k_1c_1, k_2c_2, and k_3c_3 of these planes normal to the stagnation line. For the positions k_1c_1 and k_2c_2, the effective two dimensional flow is that of a planing semi-infinite flat plate as analyzed by Wagner (1932). As shown on the sketch of Fig.6, the velocity component Vn approaches the plate at an effective angle of attack τ 'relative to the level water surface. This velocity component stagnates at the stagnation line. Just forward of this point a thin sheet of fluid, referred to as the spray sheet, is formed and flows along the bottom in a forward direction at a velocity equal to the approach velocity Vn. Based upon Wagner's analysis, Pierson and Leshnover (1948) approximated the spray thickness, δ, as a fraction of the wetted length (lm) measured to the spray root. Thus:

$$\frac{\delta}{lm} \approx \frac{\pi \tau_{RAD}^{\ 2}}{4 + 2\pi\tau_{RAD}} \qquad \text{Eq. 4}$$

where τ_{RAD} is the trim angle in radians.

Thus, for a trim angle of 12 degrees (0.21 radians), δ is 2.5 % of lm and is directed upward along the semi-infinite plate at a velocity equal to Vn. Since l increases as the two-dimensional k-c sections approach the chines, the spray thickness also increases as the distance outboard of the keel increases.

The initial trajectory angle of the spray depends upon the initial extent of the upper end of the plate above the water surface. The sketches on Fig.6 show that this distance decreases as the two dimensional planes approach the chines. Green (1935) considered plates of both finite and infinite length planing on fluids of infinite and finite depth. The sketches on Fig.7 illustrate the flow patterns for an infinite length plate as treated by Wagner and for the case where the leading edge of the plate is in the proximity of the free water surface as treated by Green. It is seen that the spray trajectory angle becomes considerably larger than the trim angle when the leading wedge of the plate approaches the free surface. When the leading edge is submerged, the trajectory angle increases further and the flow pattern appears as for a fully ventilated flat planing surface.

Applying Green's formulas, Fig.8 has been prepared to show the variation in spray trajectory angle relative to the horizontal water surface (expressed as sin ($\gamma + \tau$)), with increasing ratio of wetted length to total length of the two dimensional plate. When the sine of this angle is 1.0, the angle is 90 deg. and the spray direction is normal to the free water surface. It is seen, that for a trim angle of 10 deg. and for ratios less than 0.90, the spray trajectory angle is constrained by the plate and is equal to the trim angle of the flat planing surface. When the ratio becomes larger than 0.90, (such as at sections approaching the chines), Vn is no longer constrained to move along the bottom, and a rapid increase in trajectory angle results as the spray sheet departs from the leading edge of the plate.. In fact, the trajectory of Vn attains a maximum value of 90 deg. relative to the level water surface and then decreases for further increases of the wetted length of the plate as the chine is approached. As shown in Fig. 8, all this happens within a very short distance inboard of the chine as measured along the stagnation line. For trim angles greater than 10 deg. it is seen that the increase in trajectory angle with increased wetted length is noticeably less rapid but also attains a maximum value of 90 deg. This circular distribution of the trajectory angle of Vn (in a plane normal to the stagnation line) from a value equal to the running trim angle for sections at large inboard distances from the chine to a maximum value of 90 deg as the chine is approached and then to reduced values as the chine is further approached) is shown in Fig. 9. For the purposes of this illustration, the changes in trajectory angle of Vn are assumed to occur relative to a single point on the stagnation line. As is shown in a subsequent section of this report, when combined with the velocity Vs along the stagnation line, the combination forms the basis for the development of the three-dimensional cone- shaped blister that typifies the appearance of the main spray at its origin.

A brief series of Davidson Laboratory model tests of a finite length flat plate planing at an angle of 15 deg. and at a Cv = 4.0 were made to examine the appropriateness of the results of the Green's analysis. Tests were made at static wetted length / total length of plate ratios varying from 0.81 to 0.92. Fig.10 contains photographs of the spray trajectories corresponding to these test conditions. It is seen that theoretical conclusions of Green are qualitatively confirmed. Specifically, for a ratio of static wetted length / total length ratio of 0.92 the spray indeed bends around the leading edge of the plate and has a trajectory angle relative to the trimmed flat plate of approximately 118 deg. or 118 + 15 = 133 deg. relative to the level water surface This is in sharp contrast to the infinitely long flat plate case where the spray direction is equal to the trim angle of the plate (in this example 15 deg. relative to the level water surface).

Using the above observations it is now possible to define the origins of the whisker spray and main spray for a three-dimensional planing hull.

Spray Patterns for Three-Dimensional Planing Hulls

Whisker Spray. As shown on Fig.6, for two-dimensional sections normal to the stagnation line, the oncoming velocity component Vn is deflected from the stagnation line and is redirected forward along the bottom at the same velocity Vn. In actual three-dimensional flow, the velocity component along the stagnation line, Vs, (in a direction from keel to chine) is added vectorially to the velocity component Vn. As shown by the dashed vectors on Fig.11, the resultant velocity V then makes an angle α relative to the stagnation line. This is exactly equal to the angle between the free-stream velocity and the stagnation line. This principal that "the angle of incidence of the free stream is equal to the angle of reflection of the spray relative to the stagnation line" was suggested by Pierson and Leshnover (1950).

This analytical conclusion is supported by experimental data as noted in a paper by Savitsky, Delorme, and Datla (2007). They refer to flow studies along the bottom of a planing hull wherein the hull was coated with a so-called soluble "turbulence detection paint". As shown on the photograph in Fig.12, the direction of the flow in the area forward of the stagnation line is clearly identified by streaks in the soluble bottom paint and indeed confirms that the angle of reflection of the whisker spray velocity relative to the stagnation line, is equal to the angle of incidence of the free stream velocity relative to the stagnation line. This experimental observation provides credibility to the approach undertaken in this study to explain the origin of the spray patterns on planing hulls. A subsequent section of this paper applies this approach to also characterize the main spray.

An important characteristic of the whisker spray is that it leaves the chine at an angle that is equal to the local geometric angle of the hull bottom relative to the level water surface. For conventional combinations of trim and deadrise, this hull bottom angle is relatively small and, consequently, the whisker spray, which follows a ballistic trajectory after leaving the chine, does not achieve large heights above the water surface. Furthermore, since the whisker spray is composed of thin, light droplets of fluid it is readily deflected by the moderate alterations to the chine geometry.

The length of the whisker spray, Lws, measured forward along the chine from the stagnation intersection with the chine is given by the following equation:

$$Lws = \frac{b \tan \beta}{\pi \tan \tau} - \frac{b}{2 \tan(2\alpha)} \qquad \text{Eq. 5}$$

The leading edge of spray sheet along the bottom makes an angle, α, relative to the stagnation line and 2α relative to the keel (see Fig.11). The angle α has been defined previously.

Main Spray (Origin and Description). Main spray is the more important of the two distinct spray patterns shown on Fig.1 because it is more likely to impact adjacent structure and increase the resistance of the craft. Its appearance, at moderate speeds, initially resembles a continuous blister of fluid in the form of a cone whose apex is in the vicinity of the stagnation line intersection with the chine. As the speed increases, the blister becomes unstable, and breaks-up into a dense distribution of droplets of water with large trajectory angles and a velocity equal to the speed of the craft. This spray of droplets becomes aerated, and when seen on full-scale planing craft has a milky-white appearance (see Fig. 13). Main spray can cause structural damage and increase the hull resistance when impacting sections of the hull that are in the path of its trajectory. This is particularly evident with planing catamarans (with symmetrical hulls) and water-based aircraft. The following discussion provides a qualitative description of the hydrodynamic flows that lead to the development of the main spray.

For the previously described two-dimensional planes normal to and near the chine terminus of the stagnation line, i.e., section $k_3 c_3$, a sharp change in the flow pattern takes place. This is because the effective two-dimensional section becomes a surface of finite length whose leading edge is in close vicinity to the water surface and whose flow patterns are described by Green and confirmed by the experimental results of the present study. As previously shown, both the spray thickness and its trajectory angle increase rapidly for sections approaching the chine. In fact, the two dimensional velocity component of the spray, Vn, actually attains a 90 deg, trajectory angle relative to the level water surface.

For the three-dimensional planing hull the Vn component of the velocity, (V sin α) is combined vectorially with the velocity component Vs, (V cos α), along the stagnation line so that the resultant velocity of the outboard directed spray is equal to the free stream velocity V. Consider a plane perpendicular to the stagnation line, and recall (from Fig.9) that the circular distribution of the direction of Vn relative to the free water surface varies from a small value (trim angle) to a maximum of 90 deg. and then decreases as the chine is approached—all this occurs within a relatively small distance

in the vicinity of the chine intersection with stagnation line. The combination of the vectors Vn and Vs leads to a cone shaped main spray pattern with its apex at the intersection of the stagnation line and the chine (Fig. 9). Further, its maximum height is located in the plane where Vn is at an angle of 90 deg. relative to the level water surface.

The above representation of the velocity components neglects the effects of deadrise angle and trim on the initial spray trajectory angle relative to the level water surface. It is nonetheless useful since it allowed for a simplistic description of the spray formation process. The following section includes the deadrise and trim effects.

Main Spray (Trajectory). The maximum trajectory angle of the main spray velocity relative to the level water surface is determined by the addition of the following three components.

1) The angle α (between the stagnation line and keel) as measured in a plane perpendicular to the centerline of the hull. Recall from Eq. 1 that:

$$\alpha = Tan^{-1}\left(\frac{\pi}{2}\frac{\tan\tau}{\tan\beta}\right) \qquad \text{Eq. 1}$$

2) The effective angle of deadrise, (βe), measured in a plane normal to the bottom and along the stagnation line. It can be shown that:

$$\beta e = \tan^{-1}(\sin\ \alpha\ \tan\ \beta) \qquad \text{Eq. 6}$$

3) The geometric effect of trim angle is to reduce the trajectory angle as follows:

$$\beta t = \tan^{-1}\left[\frac{(Lk - Lc)}{ls}\tan\tau\right] \qquad \text{Eq. 7}$$

where

$$Lk - Lc = \frac{b\tan\beta}{\pi\tan\tau} \qquad \text{Eq. 8}$$

$$ls = \frac{b}{2\sin\alpha} \qquad \text{Eq. 9}$$

thus

$$\beta t = \tan^{-1}\left[\frac{2}{\pi}\sin\alpha\tan\beta\right] \qquad \text{Eq. 10}$$

The resultant maximum trajectory angle, γ, (relative to the level water surface) for the main spray velocity V is thus:

$$\gamma = \alpha + \beta e - \beta\tau \qquad \text{Eq. 11}$$

Substituting Eq. 6 and 10 into Eq. 11

$$\gamma = \alpha + \tan^{-1}(\sin\alpha\tan\beta) - \tan^{-1}\left[\frac{2}{\pi}\sin\alpha\tan\beta\right] \qquad \text{Eq. 12}$$

Simplifying

$$\gamma = \alpha + \tan^{-1}\left[\left(1 - \frac{2}{\pi}\right)\sin\alpha\tan\beta\right] \qquad \text{Eq. 13}$$

The initial velocity of the main spray trajectory as it departs from the chine is the free-stream velocity V (this follows from an application of the Bernoulli equation). Its direction relative to the chine in a horizontal plane follows the stagnation line which makes an angle, α, relative to the chine line. This was confirmed by model tests, which are described in the test section of this paper.

Maximum Height of Main Spray. Combining the maximum trajectory angle, γ, with the free-stream velocity. V, results in the maximum value of the initial vertical component of the main spray velocity Vv.

$$Vv = V \sin\gamma \qquad \text{Eq. 14}$$

The maximum height of the main spray (Z) is calculated in accordance with basic trajectory equations. Thus;

$$Z = \frac{Vv^2}{2g} = \frac{V^2 \sin^2\gamma}{2g} \qquad \text{Eq. 15}$$

To normalize this expression, substitute the following definitions:

$$Z' = Z / b$$

$$Cv = \frac{V}{\sqrt{gb}}$$

so that;

$$\frac{Z'}{Cv^2} = \frac{1}{2}\sin^2\gamma \qquad \text{Eq. 16}$$

This equation is plotted on Fig 14. Thus, for a given beam, speed, trim angle and deadrise, the maximum height of the main spray is easily obtained from this Figure.

Longitudinal and Transverse Location of Maximum Height of Main Spray. These locations can also be computed by the use of the basic trajectory equations. Specifically, it has been shown that the resultant velocity of the spray is equal to the free stream velocity, V, and has a trajectory angle, γ, relative to the level water surface. This results in a maximum spray height Z as shown in the previous section of this report. The time, $t_{m,}$ to reach this maximum height is:

$$t_m = \sqrt{\frac{2Z}{g}} \qquad \text{Eq. 17}$$

The distance, Ltr, from the intersection of the stagnation line with the chine to the point of maximum spray height, as measured in the horizontal plane, is shown on Fig.15 A and is equal to:

$$Ltr = t_m V \cos\gamma \qquad \text{Eq. 18}$$

Substituting equations 15 and 17 into equation 18 and simplifying

$$Ltr = \frac{V^2}{g}\sin\gamma\cos\gamma \qquad \text{Eq. 19}$$

normalizing;

$$\frac{Ltr}{Cv^2 b} = \sin\gamma\cos\gamma \qquad \text{Eq. 20}$$

It follows then, that since the spray trajectory makes an angle, α, relative to the chine, the longitudinal distance, X', measured in a horizontal plane, from the stagnation line intersection with the chine to a point opposite the maximum height of the spray is:

$$X = Ltr\cos\alpha \qquad \text{Eq. 21}$$

normalizing;

$$\frac{X'}{Cv^2} = \sin\gamma\cos\gamma\cos\alpha \qquad \text{Eq. 22}$$

Where X' =X/b

Likewise the transverse distance, Y, between the point of maximum spray height and the side of the hull is:

$$Y = Ltr \sin\alpha \qquad \text{Eq. 23}$$

So that;

$$\frac{Y'}{Cv^2} = \sin\gamma \cos\gamma \sin\alpha \qquad \text{Eq. 24}$$

Where Y' = Y/b

The quantities X'/ Cv^2 and Y'/ Cv^2 are plotted on Fig 15B as a function of deadrise angle with trim angle as a parameter.

It is important to remember that X', and Y' are dimensions relative to the location of the maximum height, Zmax, that is located on the centerline of the main spray geometry. Since this analysis is based upon the application of kinematic considerations, the actual profile of the spray height along the centerline of the main spray can be calculated using standard trajectory equations

EXPERIMENTAL STUDIES

The experimental investigations performed in this study of the spray patterns associated with planing surfaces included basic explorations to identify the origin of the spray patterns and also detailed measurements to relate the main spray geometry with hull deadrise, running trim angle and speed.

Exploratory Tests

Dye Injection Tests. To define the division of the undisturbed water surface into the whisker and main sprays, a series of observations were made of their steady state patterns when a blue dye stream was deposited on the water surface at various locations forward of and alongside the towed model. The dye was carried in a hopper attached to the towing carriage and was released as a continuous, thin, liquid stream. The locations at which the dye was released onto the free water surface are shown on Fig. 16. The test model was a 5 inch beam, 20 deg deadrise hull that was towed at a fixed trim angle of 8 deg, a Cv of 3.00 and a mean wetted length beam ratio of 2.51. An analysis of the resultant trajectories of each of these dye streams provided the following observations relative to the origin of the spray patterns.

The dye was first introduced at position #1 (intersection of the stagnation line with the chine) to review the assumption that the main spray issues from a single small region on the chine. As had been expected, the entire main spray blister became colored blue. When the dye injection point was moved slightly forward to position #2 (in the area of the whisker spray) the main spray was uncolored and streaks of blue appeared in the area of the whisker spray surrounding the point of dye injection. The blue dye stream was then injected at positions aft of the stagnation line intersection with the chine and alongside the chine (positions #3 and #4). In these positions, the main spray remained uncolored and the blue dye appeared as a thin stream in the wake aft of the test model.

The hopper was then moved to a position 2 beams ahead of the wetted keel length and dye streams were introduced onto the water surface at positions #5, #6, #7, #8, #9, and #10. In position #5, (at the extension of the keel line), occasional streaks of blue appeared in the whisker spray but the main spray was uncolored. A major portion of this dye appeared as a blue streak starting at the transom and running aft along the longitudinal extension of the hull centerline. At position #6 substantial areas of the whisker spray were colored but the main spray and wake remained uncolored. When the dye was released at positions #7, #8, and #9 the main spray was colored but the whisker spray and trailing wake remained uncolored. .For position #10 both the whisker and main spray were uncolored A thin blue streak line parallel to the chine appeared on the water surface and extended from the point of release of the dye to well aft of the model transom.

The conclusions from this exploratory dye study reaffirmed the conviction that the main spray blister originates at a small region at the intersection of the stagnation line with the chine. It also showed that:

- The undisturbed surface fluid ahead of and along the centerline of the model appears only in the wake aft of the transom.
- The undisturbed surface fluid ahead of the model and for a distance of approximately 0.40 beams outboard of the keel appears in the whisker spray.
- The undisturbed surface fluid lying in a transverse band approximately 0.10 beams on either side of the chine appears in the main spray.
- Any free surface fluid further outboard of the keel than 0.70 beams does not contribute to either spray formation.

Spray Dam Tests. Although the dye tests did show that the main spray originates from a local position at the intersection of the stagnation line with the chine, it was considered important to verify this conclusion further since *casual observations of the main spray blister on a high speed planing hull give many the mistaken impression that water issues along the entire wetted chine length to form the main spray*.

To this end a thin metal plate 0.20 beams long was mounted on the starboard side of a 20 deg. deadrise hull and extended 0.05 beams below the chine. (Fig.17). The longitudinal position of the spray dam relative to the transom was varied. Tests were conducted at a fixed heave and a fixed trim angle of 8 deg. The model was towed at a constant speed coefficient, Cv = 3.00.

Observations of the spray patterns indicated that the longitudinal location of the spray dam had no effect on the spray appearance until the plate was moved to the stagnation line intersection with the chine. At this point, nearly the entire main spray blister was suppressed by the small plate. This is illustrated on Fig. 17 which presents photographs of the main spray with and without the small plate attached to the chine at its intersection point with the stagnation line. The main spray formation on the port side (which did not have an attached spray dam) is essentially identical in both photographs. When the local spray dam was moved forward of the stagnation line intersection with the chine, the main spray blister was undisturbed but a deflection of the whisker spray took place in the area of the spray dam. Hence, the tests with the spray dam confirm the results of the dye tests i.e. that the main spray originates at a local point on the chine.

To demonstrate still further that the main spray blister originates in a small region of the stagnation line intersection with the chine, observations were made of the spray when the wetted chine length was zero, precluding the existence of long wetted chine lengths. The main spray pattern for this condition, shown on Fig.18, was found to be identical to the spray pattern for chine wetted lengths of 2.5 beams; hence again substantiating the conclusion that the origin of the main spray is local and that fluid flow in transverse sections normal to the keel and aft of the stagnation line intersection with the chine do not contribute to the development of the main spray.

Several published theoretical papers, i.e. Kihara (2006) and experimental results, i.e. Kikuhara (1960) are based on 2-D slender body approximations (in transverse sections normal to the keel) to study the spray patterns of wedges penetrating the water surface at constant vertical velocity. As expected, their results can be applied to the 3-D case where the stagnation line angle relative to the keel (α) is small, since this geometry more closely resembles the 2-D slender body case. It is recommended that studies intended to expand 2-D results to the 3-D case be continued.

Flow Directions of Spray Patterns. Recall that the previous analysis of the characteristics of the spray patterns defined their flow directions relative to the chine. It was suggested that the angle of the stagnation line relative to the keel, α, was the controlling parameter. The direction of the outboard whisker spray relative to the chine (for prismatic hulls) was the angle 2α. The axis of the centerline of the main spray was along a continuation of the direction of the stagnation line relative to the chine and thus made an angle, α, relative to the chine. To test these conclusions a number of short tufts were attached along the length of the port chine and an overhead photograph was taken that showed the direction of these tufts with the model underway. Also, an underwater photograph was taken to define the direction of the stagnation line relative to the keel.

Fig.19 is the overhead photograph of the tufts. A close examination of their direction does confirm the expected directions of the fluid flow in both the whisker and main sprays,

Measurements of Main Spray Geometry

Previous Systematic Spray Study. Savitsky and Breslin (1958) conducted a series of tests on four prismatic models with deadrise angles of 0, 10, 20, and 30 degrees. The models were towed behind a wind screen and measurements were made of the maximum height and lateral position of the spray blister prior to its break-up into high velocity droplets. Tests were made over a range of speed coefficients and high trim angles appropriate to the operation of seaplanes and not planing hulls. All tests were made at a mean wetted length/beam ratio $\lambda = 2.5$ since it was found that

the spray heights were independent of λ. Unfortunately, the distribution of the results of that study was limited to the seaplane community and hence are not well known to designers of planing hulls. Some of their basic conclusions are however contained in the present report which is directed mainly to planing craft designers.

Major departures from the Savitsky-Breslin (1958) experimental effort are that the present experimental study is conducted without a wind screen; spray heights are measured relative to the top of the spray droplets; and both the longitudinal and lateral locations of the maximum spray height are measured.

Test Models. Three constant deadrise models having 9-inch beams and deadrise angles of 10, 20, and 30 degrees were tested. They were constructed of 3/8" Lexan. The 10 and 20 degree models, which had been used for previous studies, were painted white and were striped with black marks spaced every inch along the entire chine length (see Fig. 20). There was a 3/8" x 1/16" relief cut into their chines to assure complete separation of flow from the model when underway. These models were 36' long. The 30 degree model, which was constructed specifically for these tests, was made 6" longer to allow for the longer wetted lengths of keel associated with higher deadrise angles. This model was constructed with especially sharp chines to assure complete separation of flow. For all models the pivot attachment point to the towing carriage was 13" forward of the transom.

Test Facility and Test Conditions. Tests were conducted in the Davidson Laboratory Tank No.3 which is 313 ft long by 16.4 ft wide, and 6.5 ft deep. All models were tested at fixed trim angles of 4, 6, and 8 degrees; at speed coefficients of 2, 3, and 4, and at a fixed mean wetted length/beam ratio of 2.5. This followed from the results of model tests conducted by Savitsky and Breslin (1958) that showed the characteristics of the main spray were independent of the mean wetted length/beam ratio. Those authors also conducted a brief series of tests with and without a wind screen towed ahead of the model to examine the possible aerodynamic effects on the geometry of the main spray. The conclusions were that, while the free air stream raised the height of intact blister nearly 20%, it had no effect on the height of the spray after it was broken up into a dense field of broken droplets of water. Hence, in the present study, all tests were conducted without a wind screen. This contrasts with the previous study wherein all tests were conducted with a wind screen.

Appearance of Main Spray in Model Tests. Prior to presenting the test data that define the main spray geometry, it is essential to describe the general appearance and behavior of the spray during model tests and to identify those quantities that were measured in the tests.

A series of side-view photographs taken from Savitsky and Breslin (1958) illustrating a typical variation in the development and appearance of the main spray as the speed coefficient is increased are shown in Fig. 21. Corresponding stern view photographs of the same test runs are presented in Fig. 22. The test model is a 20 deg. deadrise, 9 inch beam, prismatic hull operating at a large trim angle of 12 deg. No main spray formation is evident for $C_v < 1.50$. Instead, a small pile up of water is visible in the area of the chine intersection with the waterline. The stern views show a small bow wave formation attached to the model. At $C_v = 1.50$ the typical main spray blister appears as a as a thin continuous sheet of fluid. At $C_v = 2.00$ the main spray blister becomes higher and larger but still maintains its essentially continuous appearance. At $C_v = 2.50$ the spray sheet increases in height and develops an instability which is characterized by the appearance of sinusoidal oscillations (not unlike that of a flag in a breeze). This instability is similar to that described by Dundurs and Hamilton (1955) in their basic study of the stability of thin sheets. At $C_v = 3.00$ the oscillations are severe enough to form droplets of water which break off the spray blister. When the planing speed coefficient is increased to $C_v=3.50$ the spray appearance is that of broken, dense droplets of fluid whose trajectory is a continuation of that portion of the main spray that is still intact. At these high speeds the inboard surface of the main spray obscures the bow wave which had developed at low speed.

Appearance of Main Spray on Full- Scale Craft. Fig. 13 is a photograph of a planing craft operating at high speed. Notice that the spray is milky white in appearance and does not have an intact blister shape such as seen in model tests. In fact, close observation of the spray when riding the full scale craft shows the spray to be broken up into a dense cloud of aerated droplets not unlike that of the model appearance at high Cv when the model spray blister breaks up. It is believed that this breakup effect is a consequence of the reduced effect of surface tension relative to inertia forces in stabilizing the spray sheet of full scale craft. For a constant value of surface tension coefficient, the Weber number of the full scale craft is considerably larger than that of the model (increases as the square of the scale ratio). In an attempt to verify this effect, Axt (1947) added Aerosol (a surfactant) to the water in the Davidson Laboratory Towing Tank. This reduced the surface tension to approximately half of its value in plain water. He noted that the reduction in surface tension did not affect the dimensions of the main spray but did change the nature of the spray from a glassy blister to a field of droplets similar in appearance to the full-scale spray.

Visual comparisons of model and full-scale heights of the main spray indicate an acceptable similarity. Locke (1943) reviewed seven different references that included discussions of possible scale effects on spray measurements of seaplanes. He noted that although there were reported instances of differences between model and full-scale results, he

concluded that "In most reasonably conventional cases, the spray blisters on ship and model can be expected to be strikingly similar under corresponding conditions." It is nevertheless recommended that additional studies be undertaken to compare model and full-scale results under controlled and identical operating conditions.

In 1991 Tanaka, Nakato, and Araki reported the results of model tests of a series of geosim models of high speed semi-displacement craft in an attempt to determine the effects of model scale on the resistance and spray geometry of these hulls. Tests were conducted at 16 Japanese towing tanks and the model beams ranged from 3.5 in. to 35 in. All tests were conducted at a Cv = 2.1. Unfortunately there was a significant variation in the test results even when the same size model was tested in different towing tanks. For example, the 18 in. beam model ran at a trim angle of 3.6 deg. in one facility while running at a trim angle of 2.2 deg. in another facility. The corresponding spray height for the 3.6 deg test was 25 % less that the spray height for the test where the model ran at 2.2 deg. trim. This result is contrary to what is expected based on the analysis of the present study. Nonetheless, Tanaka et. al drew a mean curve through the collected data from which it can be inferred that scale effects will be minimal for model beams equal to or greater than 7 in. In the present Davidson Laboratory tests the beam of the models was 9 in. Continued controlled studies (fixed trim and deadrise angles) of the effect of model size on the spray geometry are recommended.

Spray Measurement Method. The location of the main spray apex in three dimensions was obtained photographically. Its height and transverse location were measured using still and video cameras that were mounted on an auxiliary carriage attached to the aft end of and moving with the main carriage. The cameras were located approximately 15 ft. aft of the model transom and 8 in. above the water surface (see Fig.23). This aft location of the camera minimized the perspective distortion of the spray image. A transverse reference grid was mounted on the main carriage in the proximity of the spray apex. It consisted of two vertical rods stripped at one inch intervals and a horizontal scale between them (see Fig. 24). The rods were placed on either side of the spray blister to avoid interference with the intact spray. The maximum height of the spray droplets above the level water surface was obtained from the photographs of each test run by passing a horizontal line tangent to the apex and noting its intersection with the striped vertical rods. The transverse location of the apex relative to the side of the model was measured using the horizontal scale attached to the grid.

The longitudinal (horizontal) position of the spray apex relative to the stagnation line intersection with the chine was obtained using still cameras located at the side of the tank and approximately 10 in. above the level water surface. A horizontal scale attached to the towing carriage was used as the reference for measuring this distance. (Fig. 24).

Test Results and Discussion. The three dimensions that defined the location of the spray apex are listed in Table 1. These were obtained from an analysis of the test photographs as described in the previous paragraph. The data are tabulated for each deadrise model with trim angle and speed coefficient as variables. The vertical (Z'), transverse (Y'), and longitudinal (X') distances of the spray apex are given in terms of the beam and these values are then divided by Cv^2 to test the applicability of the trajectory concept developed in the previous analytical sections of this report. Due to the unsteadiness of the spray patterns observed in the tests, the accuracy of the data is estimated to be ± 10%.

The experimental results are compared with the analytical predictions on Figures 14 and 15. The agreement is considered to be good considering that the spray geometry exhibited some unsteadiness—particularly when broken up into a dense droplet formation. Hence the simple analytical approach presented in this paper for estimating the dimensions of the main spray is confirmed.

The analytical section of this report shows that, for a given speed, the height of the spray is mainly dependent upon the angle (α) of the stagnation line relative to the keel. The larger the angle α, the higher the spray and greater the lateral distance of the apex relative to the side of the hull. Recall that the magnitude of this angle is related to the trim and deadrise angles as follows:

$$\alpha = Tan^{-1}\left(\frac{\pi}{2}\frac{\tan\tau}{\tan\beta}\right) \qquad \text{Eq. 1}$$

For small deadrise angles and large trim angles, the angle α is large. For large deadrise angles and small trim angles the angle is small. Recall that the representation of the fluid flow is taken in two-dimensional planes normal to the stagnation line and also that the free stream velocity is resolved into components normal to and along the stagnation line. The larger the angle α, the larger is the velocity component, $Vn = V\sin\alpha$, normal to the stagnation line and hence the larger is the maximum spray height, since it is proportional to Vn^2. Also, since it has been demonstrated that the apex of the main spray is in the same outboard direction as the stagnation line relative to the chine (or keel), large values of α will direct the spray further outboard than will smaller angles. However, the transverse distance of the spray apex from the side of the hull is a function of both its direction, α, and the component of velocity in that

direction, Vs = Vcosα. For typical planing boat trim angles, the transverse distance of the spray apex from the side of the hull increases as deadrise decreases down to around 10 degrees. Since the pressure in the spray is assumed to be atmospheric, the resultant velocity of the main spray is equal to the free-stream velocity V.

The data also show that for a given combination of trim and deadrise angle, the quantities X'/Cv^2, Y'/Cv^2 and Z'/Cv^2 are essentially constant and hence independent of speed. This observation further confirms the conclusion that the spray trajectory follows the path of a projectile under the influence of gravity.

The test results thus confirm the analytically derived conclusions. i.e. for a fixed value of Cv and for a given deadrise angle, the spray height increases with increasing trim angle and, for a fixed trim angle, the spray height decreases with increasing deadrise angle. Also all other planing conditions being equal, the spray apex dimensions increase as the square of the speed. Thus, knowing the speed and corresponding equilibrium trim angle for a given planing hull, (which can be estimated using the method of Savitsky (1964)), the location of the main spray apex is readily obtained from the plots on and equations in Figures 14 and 15.

Example. Consider a planing craft having the following dimensions, loading, and operating speed;

Δ	64,000 lb
LOA	65.0 ft
Beam	14.4 ft
β	20 deg
LCG	26 ft
Vk	38 kts

Applying the method of Savitsky (1964), the equilibrium conditions at 38 kts are;

Trim angle	3.3 deg
Lc =Wetted chine length	27.3 ft (forward of transom)
Lk= Wetted keel length	56.1 ft. (forward of transom)
Cv	2.98

From the plots on Figures 14 and 15;

$X'/Cv^2 = 0.28$ Then: $X = B \times Cv^2 \times 0.28 = 36$ ft

$Y'/Cv^2 = 0.07$ $Y = B \times Cv^2 \times 0.07 = 9.1$ ft

$Z'/Cv^2 = 0.038$ $Z = Bx\ Cv^2 \times 0.038 = 5.0$ ft

Thus, the maximum height of the main spray is 5.0 ft above the level water surface, is located 9.1 ft outboard of the chine and is (36.0 - 27.3) = 8.7 ft aft of the transom.

CONCLUSIONS

Analytical and experimental studies were made of the origin and characteristics of the two distinctly different appearing spray patterns associated with prismatic planing hulls. It was found that these two spray patterns, identified as “whisker spray” and “main spray”, are a consequence of the same basic hydrodynamic flow phenomenon and transform seamlessly from one into the other.

The analytical method is based on consideration of fluid flows in planes normal to the stagnation line (not unlike the aerodynamic treatment of swept-backed wings where the air flow is divided into components normal to and along the sweep angle). This is a major departure from the conventional analytical treatment of planing hulls wherein the fluid flow is taken to be in two-dimensional planes normal to the keel.

Using the orientation of the stagnation line relative to the keel as a major parameter, it is shown, and experimentally verified, that the direction of the whisker spray relative to this line is equal to the angle of incidence of the free stream velocity relative to the stagnation line. This spray sheet can be easily deflected by properly located longitudinally spray strips and hence does not present a problem to the designer.

The main spray has the shape of a conical blister with its apex located at the intersection of the chine and stagnation line. It is shown that this geometry follows from the significant increases in the volume and upward angle of the forward flow of fluid as it departs from the leading edge of the two dimensional sections normal to the stagnation line in the vicinity of the chines. Again, the orientation of the stagnation line relative to the keel has a major effect on the height and outboard orientation of the main spray relative to the hull. The height of the main spray increases as the

stagnation line angle increases. It is shown that the magnitude of this angle increases with increasing trim angle and decreasing deadrise angle. Thus, high trim angles and low deadrise angles will produce the maximum spray patterns. The analytical method also shows that the main spray height increases as the square of the velocity.

The results of several directed experiments clearly demonstrate that the main spray originates very locally at the intersection of the chine and stagnation line.

An analytical method is provided to calculate the maximum height of the main spray and its longitudinal and lateral distances from the hull. An experimental program provided model data which essentially confirmed the analytical predictions. An example is provided that illustrates the simplicity of application of the method when predicting the spray pattern for a 65 ft. planing hull.

ACKNOWLEDGEMENTS

The authors thank Stevens Institute of Technology for the use of the Davidson Laboratory towing tank and the undergraduate students Eric Giesberg, Matthew Gordon, and Alex Pollara whose enthusiastic participation and helpful suggestions contributed much to expediting the experimental phase of this study. In addition, we appreciate the interest and partial support of the T&R Committee of SNAME in encouraging this research. Also, the contributions made by Dr. John P. Breslin in the original studies of main spray conducted by the Davidson Laboratory in 1958 are gratefully acknowledged.

REFERENCES

Axt, W.C. (1947). “The Effect of Scale, Surface Tension, and Accelerations on The Main Spray Characteristics of Geometrically Similar Flying-Boat Hull Models” Davidson Laboratory, Stevens Institute of Technology, Technical Note No.59

Dundrus, J. and Hamilton,W.S. (1955). “Disintegration of Seaplane Spray and Flat Sheets” Northwestern University, Evanston, Illinois,June 1955.

Green,A.E. (1935). “The Gliding of a Flat Plate on a Stream of Finite Depth” Jesus College. Proceedings of the Cambridge Philosophical Society, Volume 31, October,1935.

Kihara, Hajime, (2006) “A Computing Method for the Flow Analysis Around a Prismatic Planing Hull” 5th International Conference on High Performance Marine Vehicles, 8-10 November, 2008, Australia.

Kikuhara,S. (1960), “ A Study of Spray Generated by Seaplane Hulls”, Journal of the Aero/Space Sciences 1960.

Locke, F.W.S. (1943), “A Method for Making Quantitative Studies of the Main Spray Characteristics of Flying Boat Hull Models” Davidson Laboratory, Stevens Institute of Technology Report No. 232

Pierson, John D. and Leshnover, Samuel (1948). “An Analysis of the Fluid Flow in the Spray Root and Wake regions of Flat Planing Surfaces” Davidson Laboratory, Stevens Institute of Technology Report No. 335, October, 1948.

Pierson, John D. and Leshnover, Samuel (1950) “A Study of the Flow, Pressures and Loads Pertaining to Prismatic Vee-Planing Surfaces” Davidson Laboratory, Stevens Institute of Technology, Report No.382, May 1950

Savitsky, Daniel (1964). “Hydrodynamic Design of Planing Hulls” SNAME Marine Technology, Vol. 1. No 1,October 1964

Savitsky, Daniel and Breslin, J.P (1958) “ On the main Spray generated by Planing Surfaces” Davidson Laboratory, Stevens Institute of Technology, Report No, 678, January, 1958

Savitsky, Daniel, Delorme, M. F., and Datla, R. (2007). “Inclusion of Whisker Spray Drag in Performance Prediction Method for High Speed Planing Hulls” SNAME Marine Technology, Vol.44, No.1, January, 2007

Savitsky, Daniel and Neidinger, Joseph,W. (1954) “Wetted Area and Center of Pressure of Planing Surfaces at Very Low Speed Coefficients” Davidson Laboratory, Stevens Institute of Technology , Report No. 493, July, 1954.

Smiley, Robert F. (1951). “A Semi-Empirical Procedure for Computing the Water-Pressure Distribution on Flat and V-Bottom Surfaces During Impact or Planing” NACA TN 2583, December, 1951

Tanaka, H., Nakato, M., Ueda,T., and Araki, S. “Cooperative Resistance Tests with Geosim Models of a High Speed Semi-Displacement Craft”, Journal of Society of Naval Architects of Japan. Vol. 169, June 1991, pp. 55-64.

Wagner ,Herbert, (1932) “Uber Stoss-und Gleitoorgauge an der Oberflache von Flussiglaseiten”, Z.f.a.M.M., Bd.12, Heft 4, August, 1932.

Table 1: Spray Apex Location

Beta deg	*Tau deg*	*Cv*	*Trans from side (beams) Y'*	*Vert from surf. (beams) Z'*	*Long'l from Lc (beams) X'*	*Broken Droplets*	*Y' / Cv²*	*Z' / Cv²*	*X' / Cv²*
10	4	2	-	-	-	No	-	-	-
10	4	3	-	1.19	2.32	Yes	-	0.13	0.26
10	4	4	3.94	1.86	6.21	Yes	0.25	0.12	0.39
10	6	2	1.44	0.69	0.87	Yes	0.36	0.17	0.22
10	6	3	3.67	2.42	2.98	Yes	0.41	0.27	0.33
10	6	4	+	+	+	Yes	+	+	+
10	8	2	1.78	1.19	0.86	Yes	0.44	0.30	0.21
10	8	3	+	3.53	3.52	Yes	+	0.39	0.39
10	8	4	+	+	+	Yes	+	+	+
20	4	2	0.44	0.14	1.16	No	0.11	0.04	0.29
20	4	3	1.00	0.31	2.16	No	0.11	0.03	0.24
20	4	4	1.28	0.69	4.82	No	0.08	0.04	0.30
20	6	2	1.00	0.32	1.68	No	0.25	0.08	0.42
20	6	3	1.78	0.94	2.12	Yes	0.20	0.10	0.24
20	6	4	2.94	1.61	5.79	Yes	0.18	0.10	0.36
20	8	2	0.78	0.60	1.99	No	0.19	0.15	0.50
20	8	3	2.78	1.61	4.21	Yes	0.31	0.18	0.47
20	8	4	+	+	+	Yes	+	+	+
30	4	2	-	-	-		-	-	-
30	4	3	0.25	0.22	1.21	No	0.03	0.02	0.13
30	4	4	0.33	0.32	1.99	No	0.02	0.02	0.12
30	6	2	0.33	0.18	0.72	No	0.08	0.05	0.18
30	6	3	0.69	0.39	2.50	No	0.08	0.04	0.28
30	6	4	+	0.65	5.61	No	+	0.04	0.35
30	8	2	0.56	0.35	1.02	No	0.14	0.09	0.26
30	8	3	1.56	0.86	3.13	No	0.17	0.10	0.35
30	8	4	+	1.21	5.69	Yes	+	0.08	0.36

- Indicates spray too small to measure using test setup

+ Indicates spray too high or broken up to measure accurately with test setup

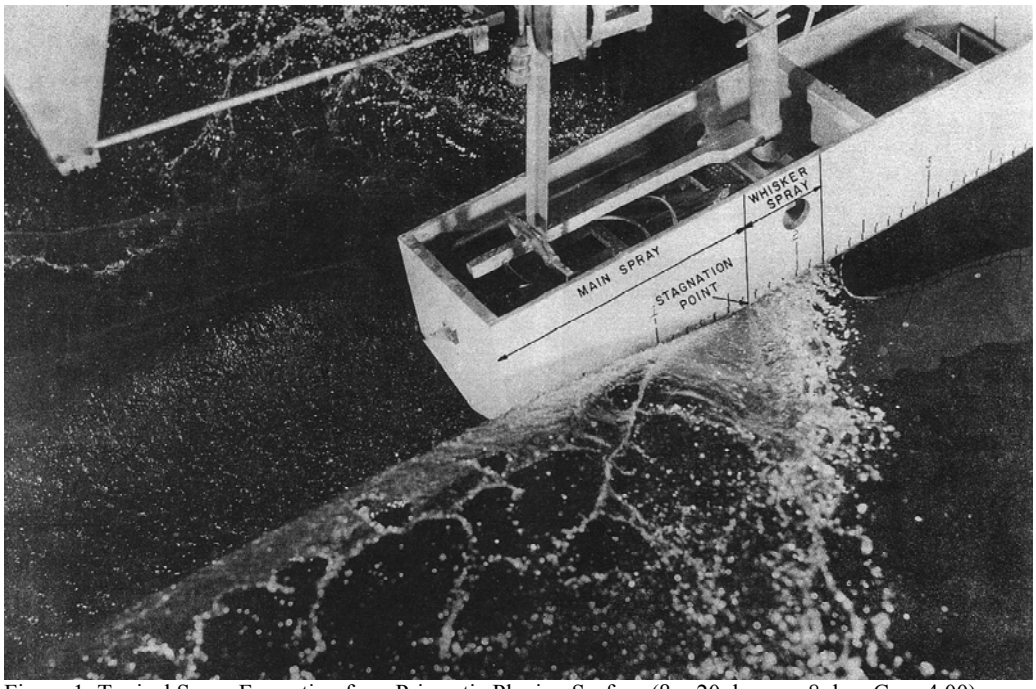

Figure 1: Typical Spray Formation for a Prismatic Planing Surface (β = 20 deg, τ = 8 deg, Cv = 4.00)

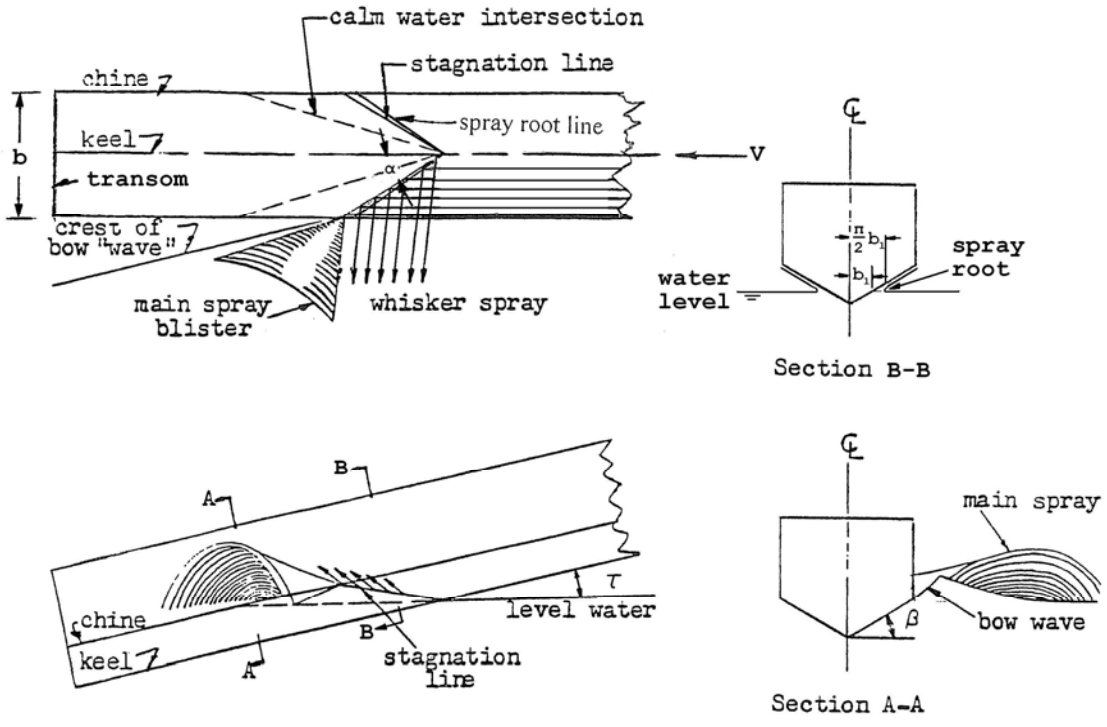

Figure 2: Graphical Representation of Spray Components

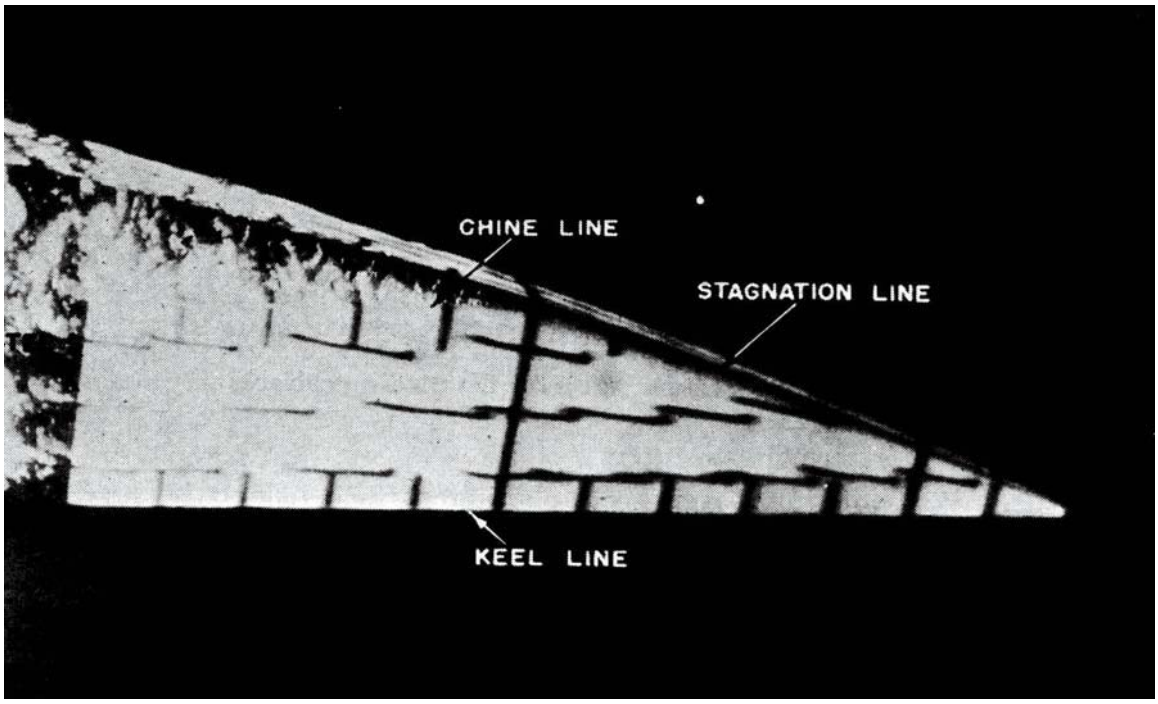

Figure 3: Underwater Photograph Showing Arrangement of Tufts over Chines Dry Prismatic Planing Hull Bottom Illustrating Direction of Fluid Flow

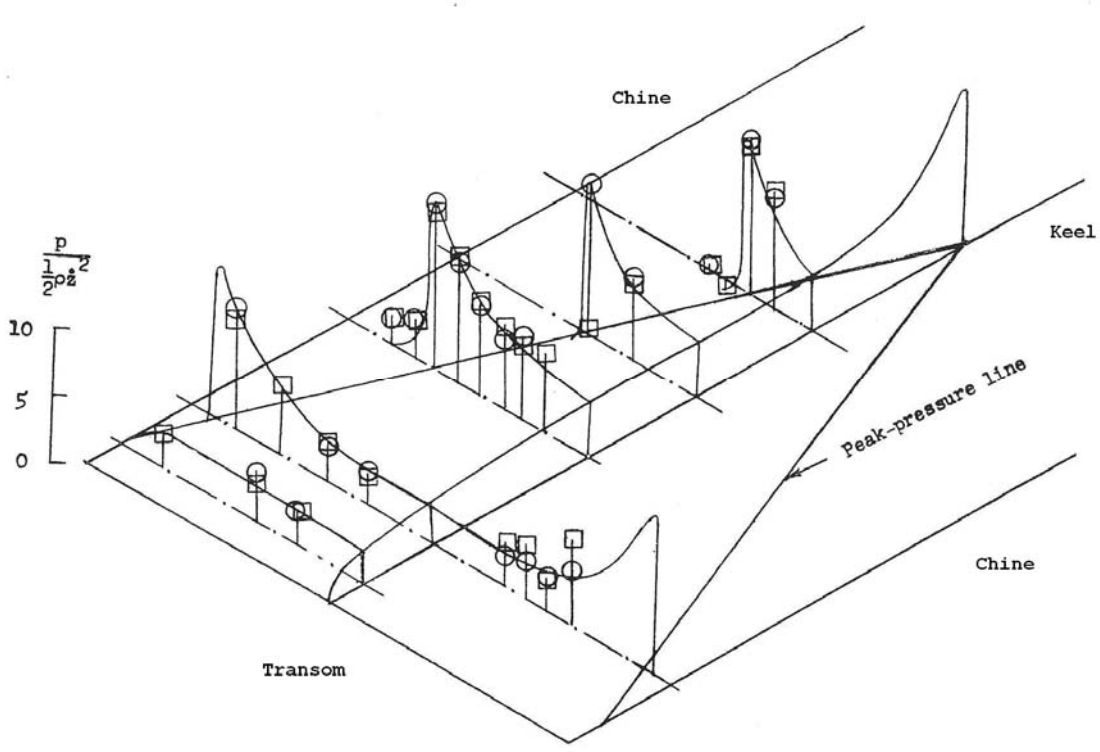

Figure 4: Pressure Distribution in Chines-Dry Region of Prismatic Planing Hull (Smiley, 1951)

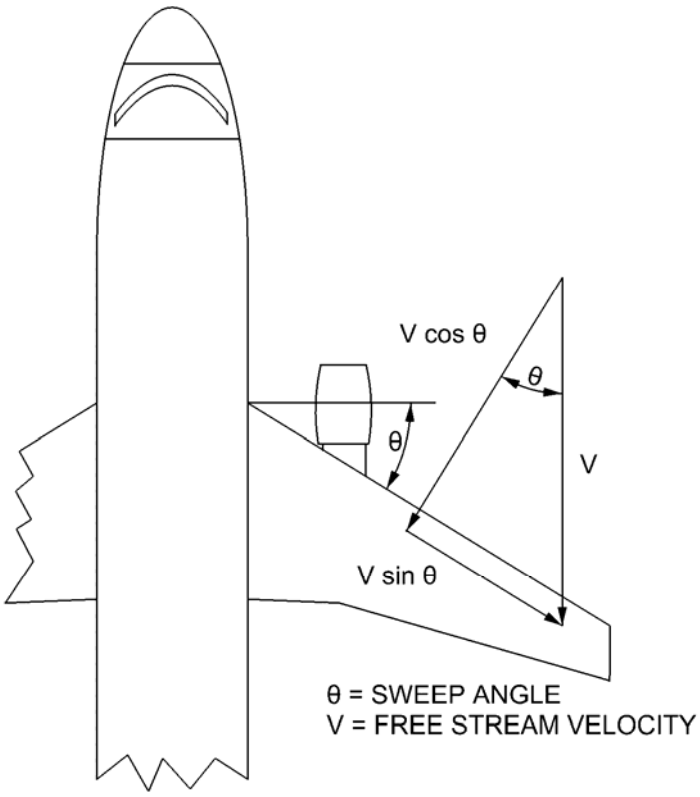

Figure 5a: Velocity Components for Swept-Back Wing

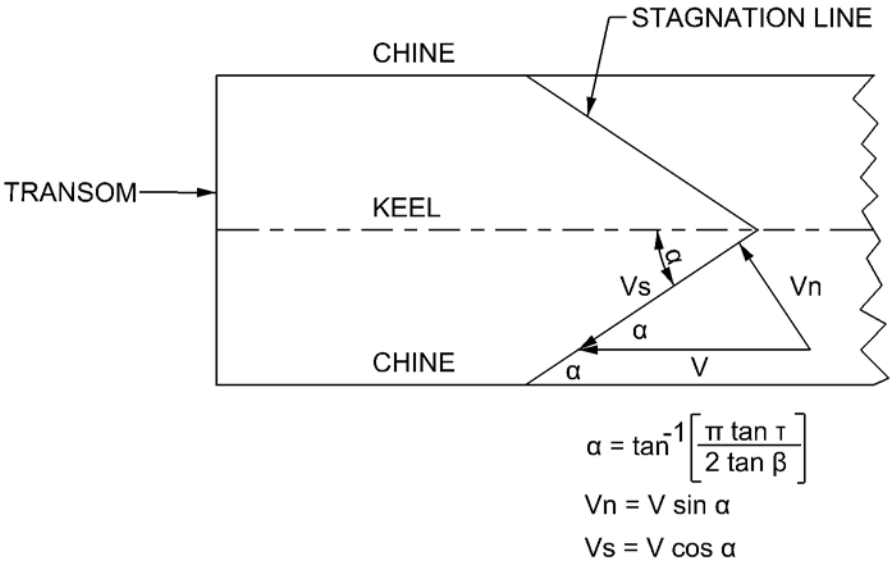

Figure 5b: Velocity Components for Planing Hull

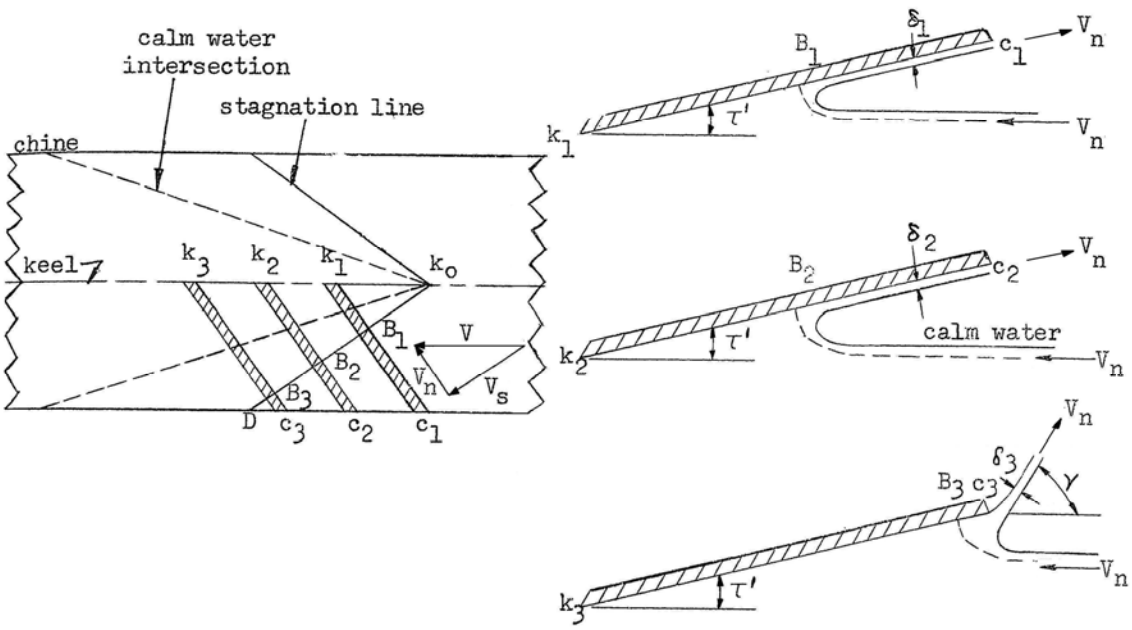

Figure 6: Two-Dimensional Flow Planes Normal to Stagnation Line

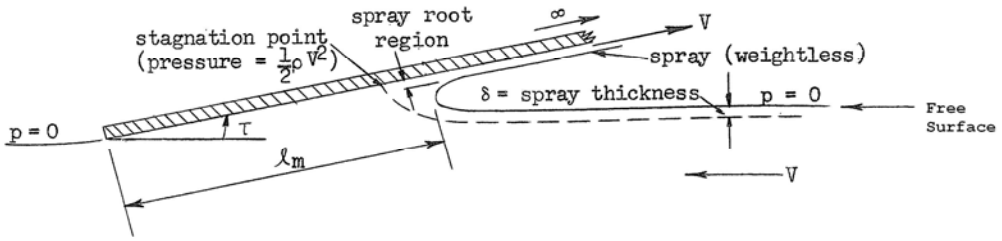

Wagner's Two-Dimensional Spray Configuration

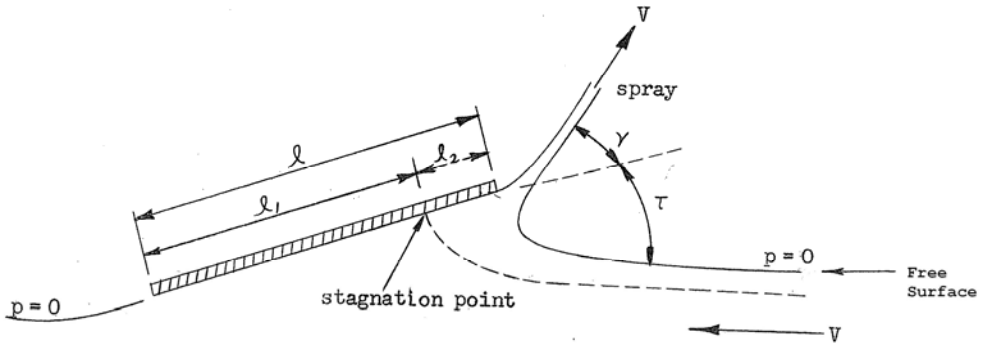

Green's Two-Dimensional Spray Configuration for Finite Length Planing Plate

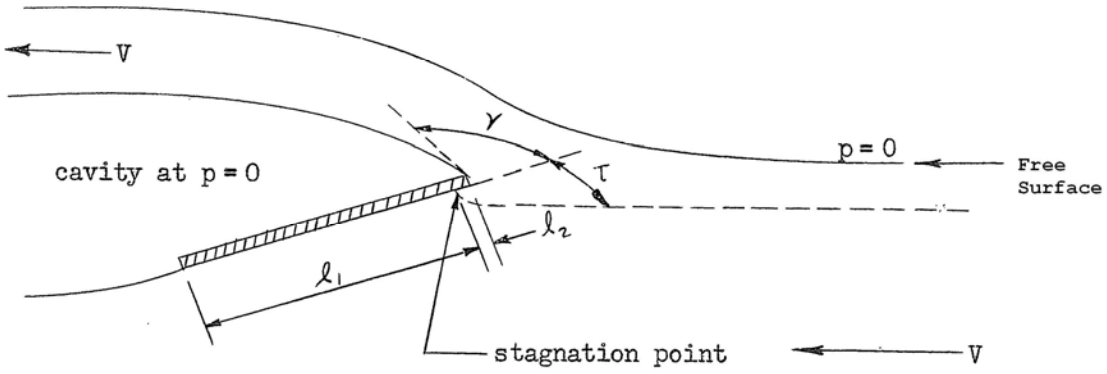

Fully Ventilated Submerged Flat Planing Plate

Figure 7: Spray Trajectories versus Location of Leading Edge of Flat Plate Relative to Level Water Surface

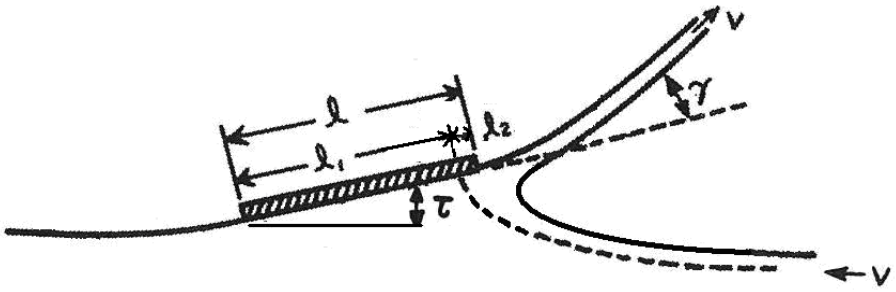

Resultant Spray Angle Relative to Level Water = τ + γ

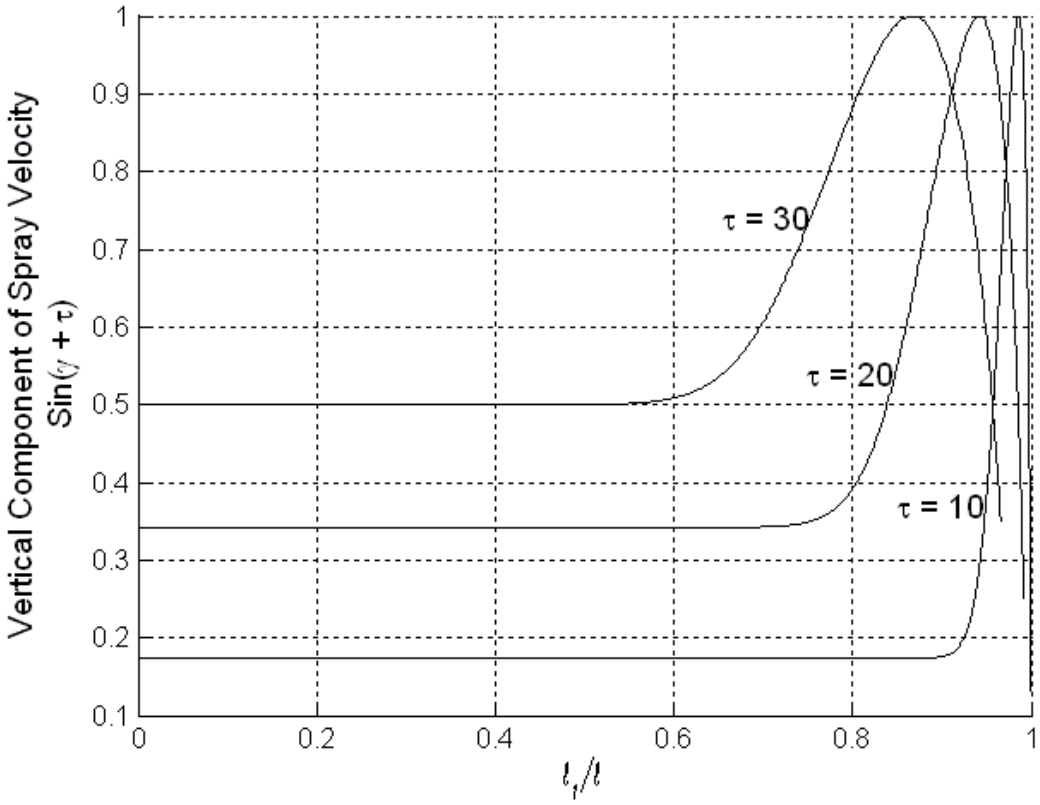

Figure 8: Variation of Spray Angle with Depth of Submergence for a Two-Dimensional Flat Plate at various Trim Angles (Green, 1936)

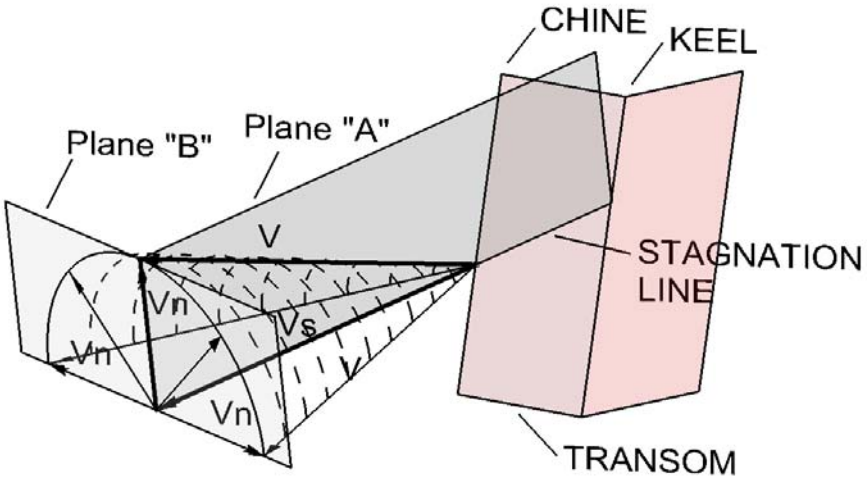

Vn is perpendicular to Vs, has a constant magnitude and varying direction and is in plane B

Vs is velocity along stagnation line, has a constant magnitude and direction, and is in plane A

V is planing velocity = vector sum of Vn + Vs

Figure 9: Illustration of Combination of Vn and Vs to Form Main Spray Blister at Chine

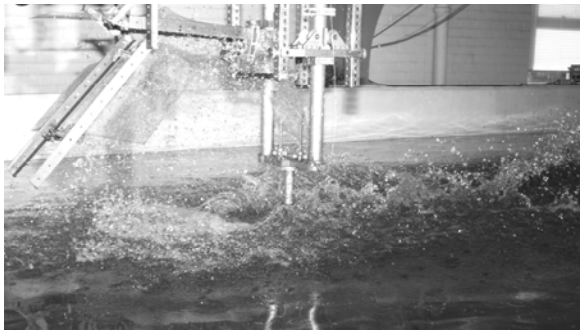

Ls/L = 81%

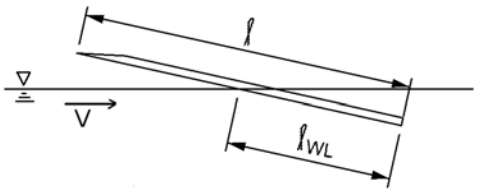

τ = 15 deg; β = 0 deg; Cv = 3.2

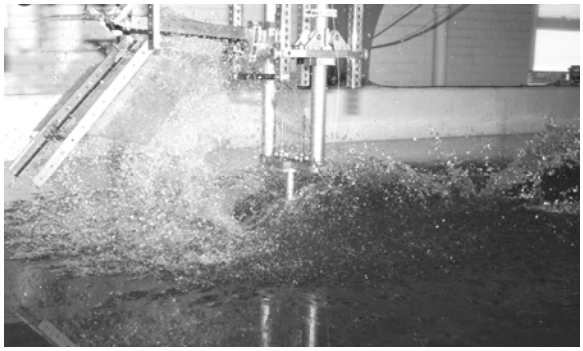

Ls/L = 85%

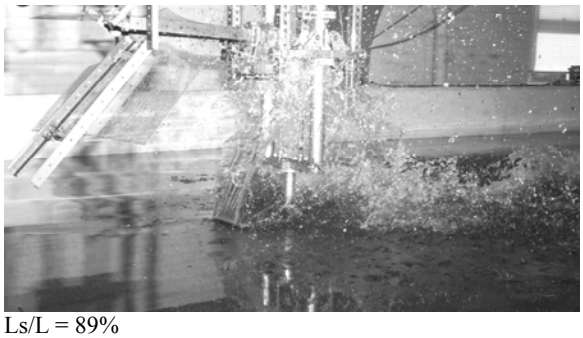

Ls/L = 89%

Ls/L = 92%

Figure 10: Planing Flat Plate with Increasing Depth of Submergence τ = 15 deg, β = 0 deg; Cv=3.2

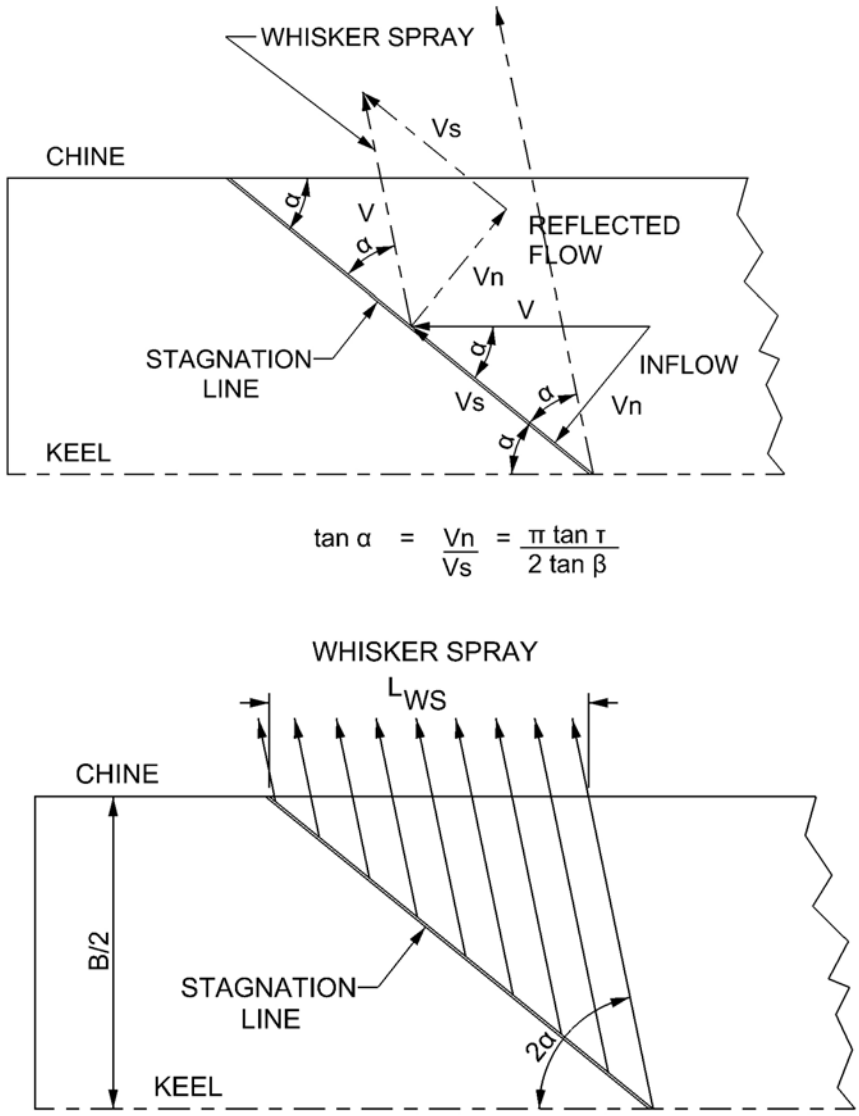

Figure 11: Formation of Whisker Spray (Angle of Incidence = Angle of Reflection)

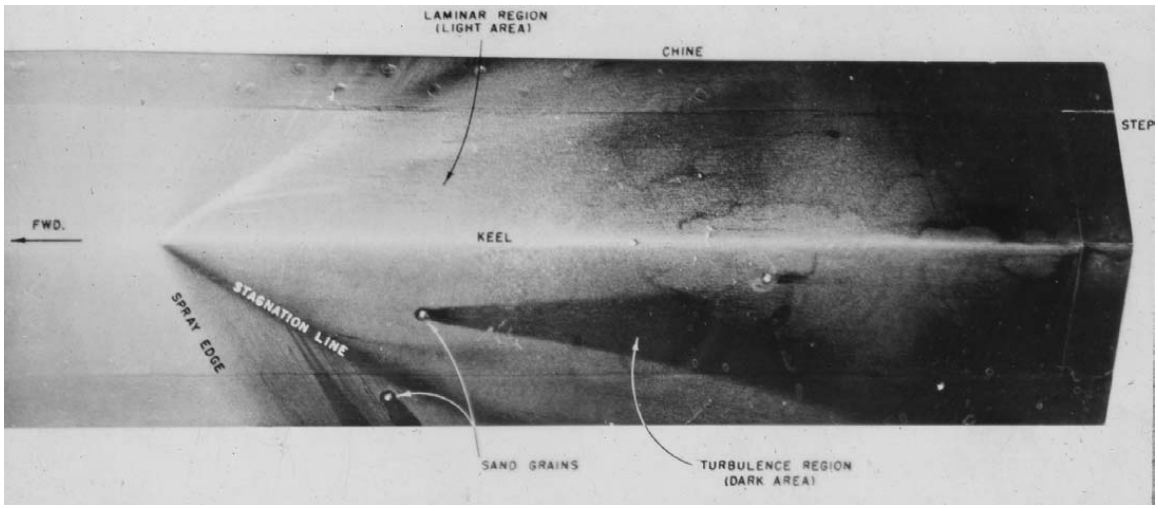

Figure 12: Underwater Photograph Showing Direction of Flow in Whisker Spray Area


Figure 13: Photo of Spray on Full-Scale Planing Craft

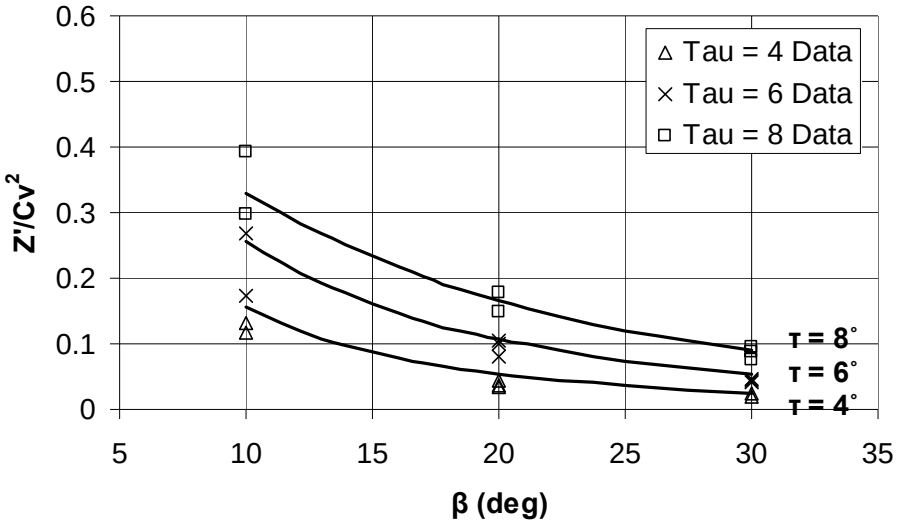

$$\alpha = Tan^{-1}\left(\frac{\pi}{2}\frac{\tan\tau}{\tan\beta}\right)$$

$$\gamma = \alpha + \tan^{-1}\left[\left(1-\frac{2}{\pi}\right)\sin\alpha\tan\beta\right]$$

$$\frac{Z'}{Cv^2} = \frac{1}{2}\sin^2\gamma$$

Figure 14: Maximum Value of Spray Height as a function of Deadrise and Trim Angle (Solid Lines Indicate Predicted Results)

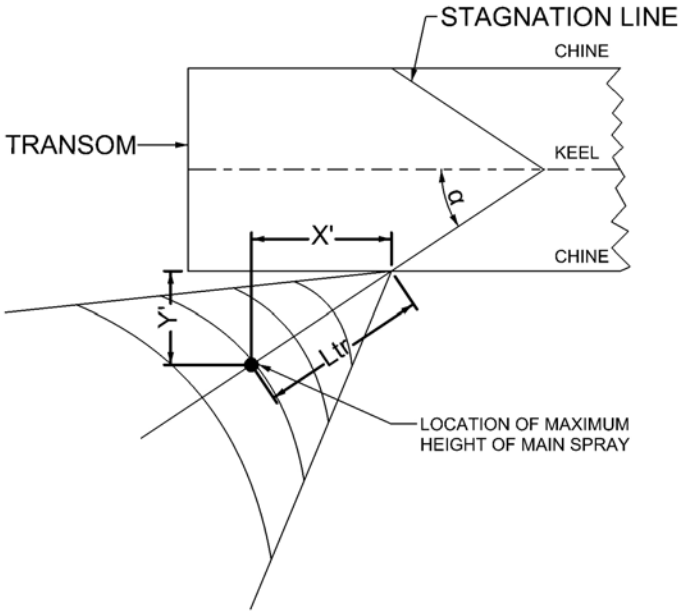

Figure 15A: Longitudinal and Transverse Location of Maximum Height of Main Spray

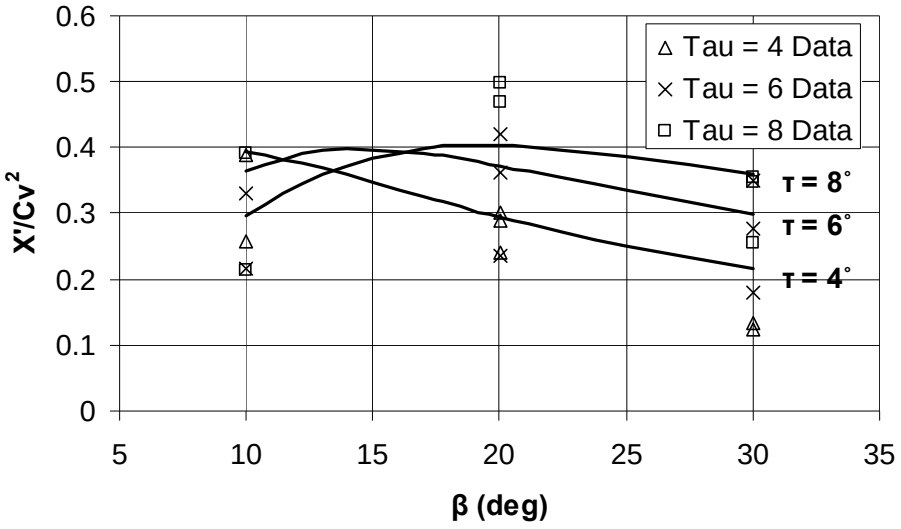

$$\frac{X'}{Cv^2} = \sin\gamma\cos\gamma\cos\alpha$$

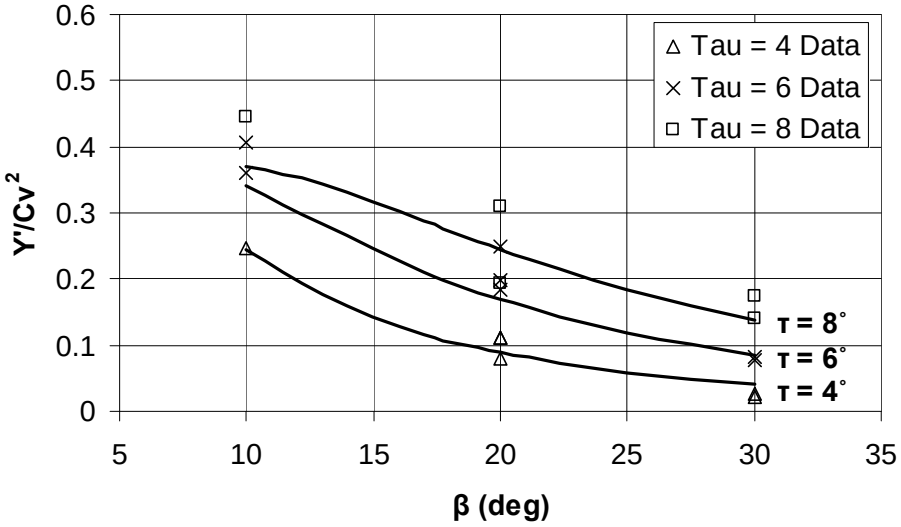

$$\frac{Y'}{Cv^2} = \sin\gamma\cos\gamma\sin\alpha$$

Figure 15B: Plots of Longitudinal (X) and Transverse (Y) Location of Maximum Height of Main Spray (Solid Lines Indicate Predicted Results)

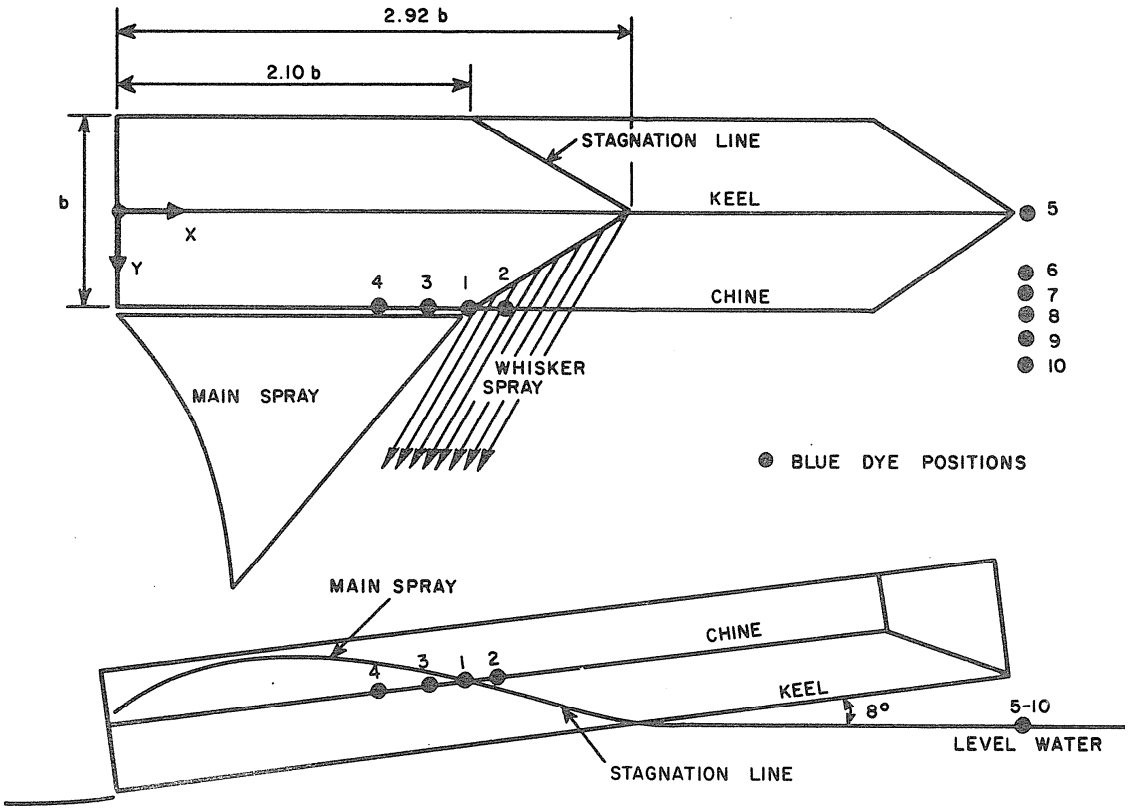

Position	x	y
1	2.10 b	.50 b
2	2.20	.50
3	2.00	.50
4	1.50	.50
5	7.80	0
6	7.80	.24
7	7.80	.38
8	7.80	.50
9	7.80	.60
10	7.80	.68

Figure 16: Location of Blue Dye Positions (Beta = 20 deg, b = 5 inch, Cv = 3.00)

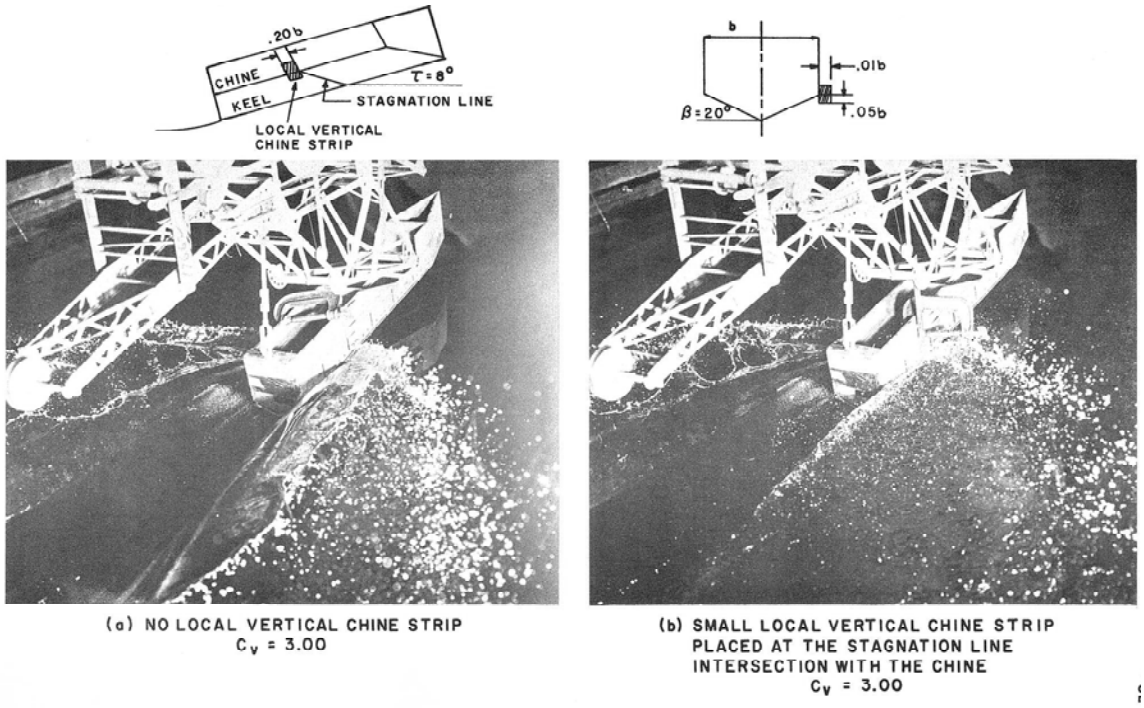

Figure 17: Effect on Main Spray Pattern of Local Vertical Chine Strip Placed at the Stagnation Line Intersection with the Chine

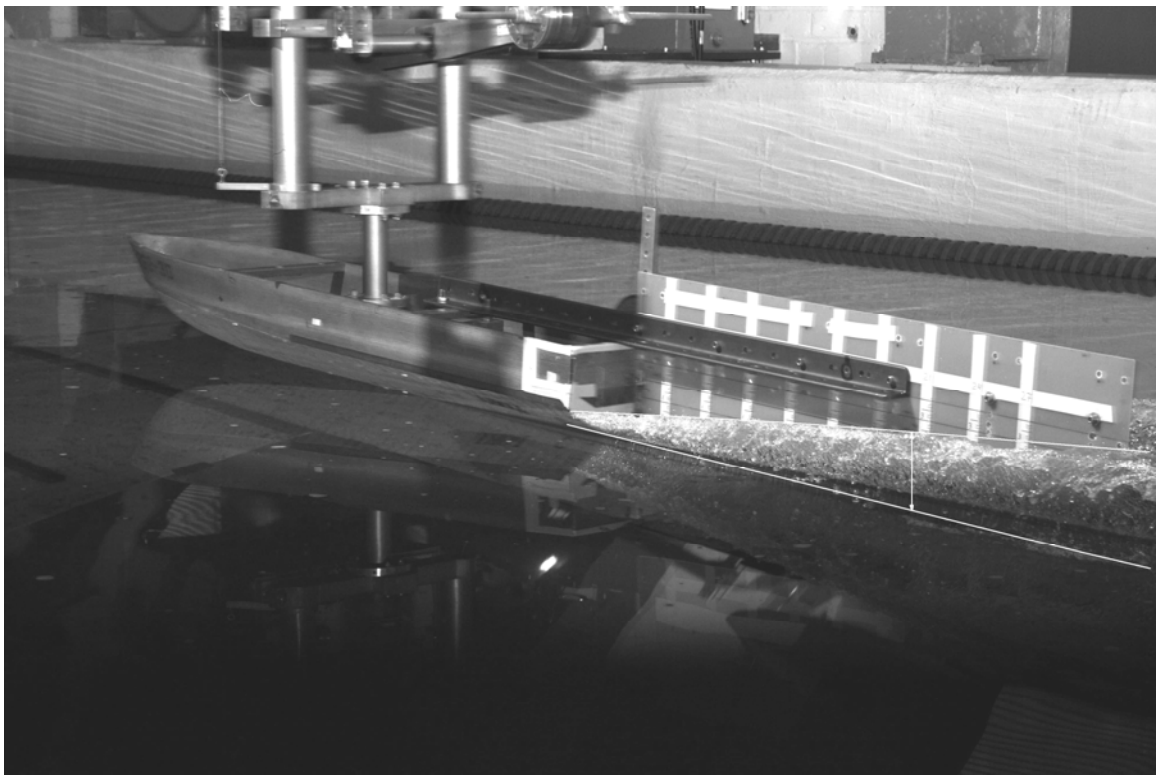

Figure 18: Spray Patterns for Short Wetted Lengths of Chine

Figure 19: Tufts Located Along Chine ($\beta = 20$, $\tau = 6$, $Cv = 3$)

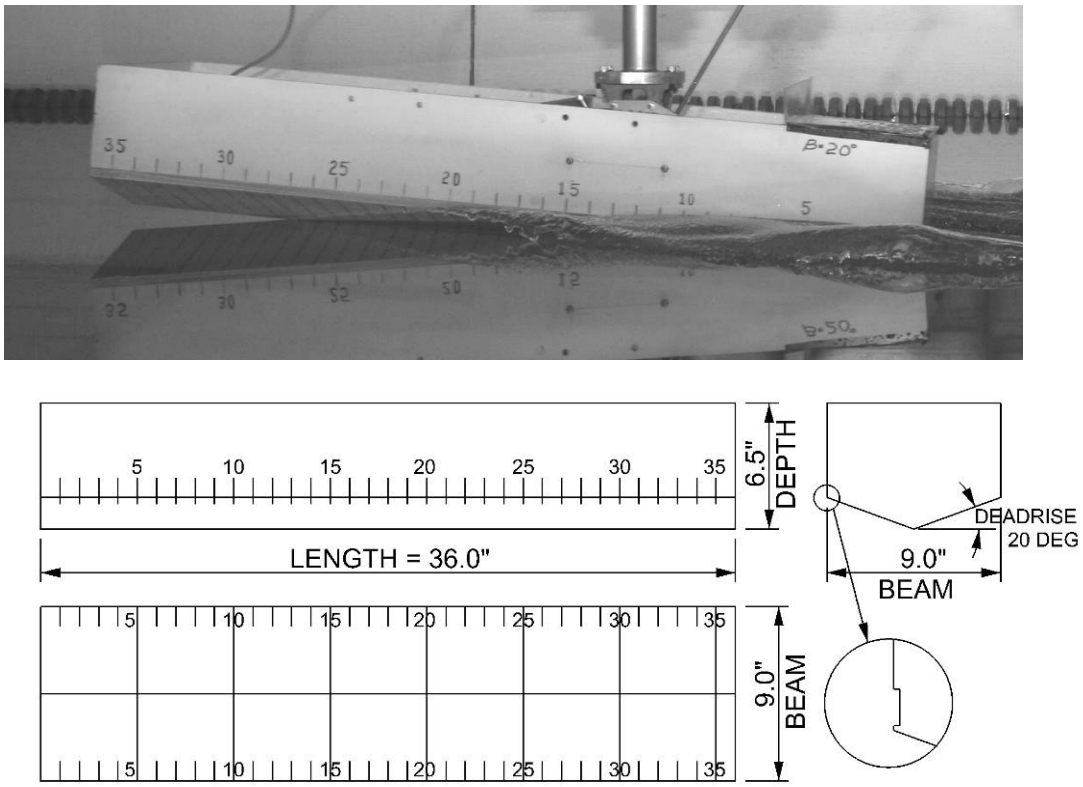

Figure 20: 20-Degree Test Model

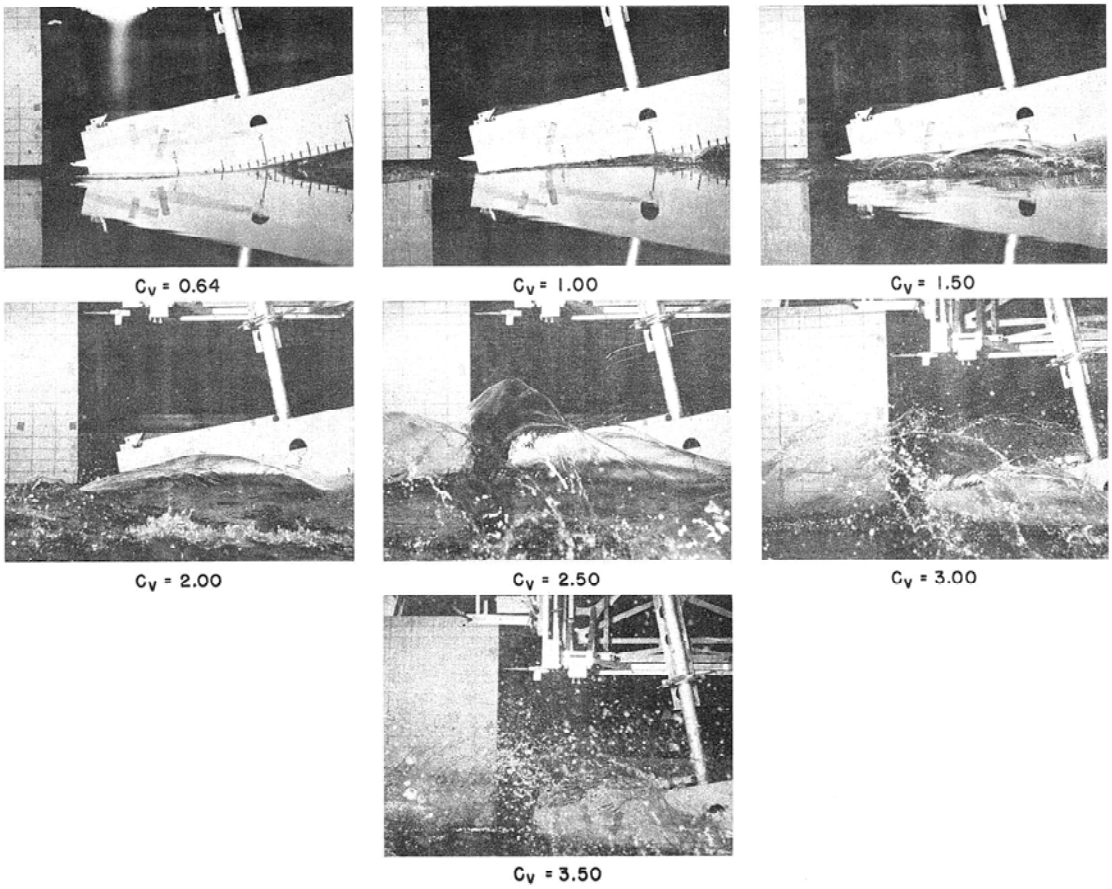

Figure 21: Variation of Main Spray Pattern with Increasing Speed Coefficient (Beta = 20 deg, Tau = 12 deg, b = 9 inch)

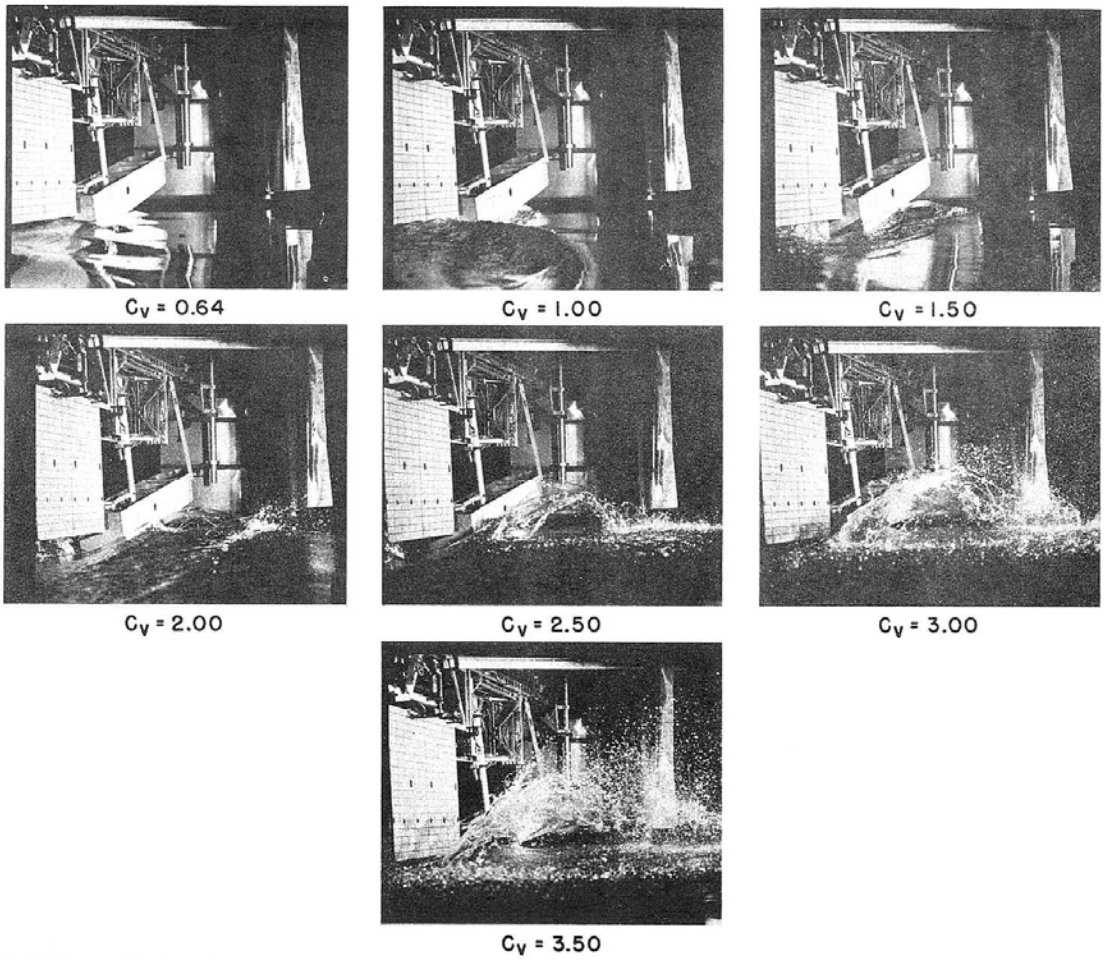

Figure 22: Variation of Main Spray Pattern with Increasing Speed Coefficient (Beta = 20 deg, Tau = 12 deg, b = 9 inch)

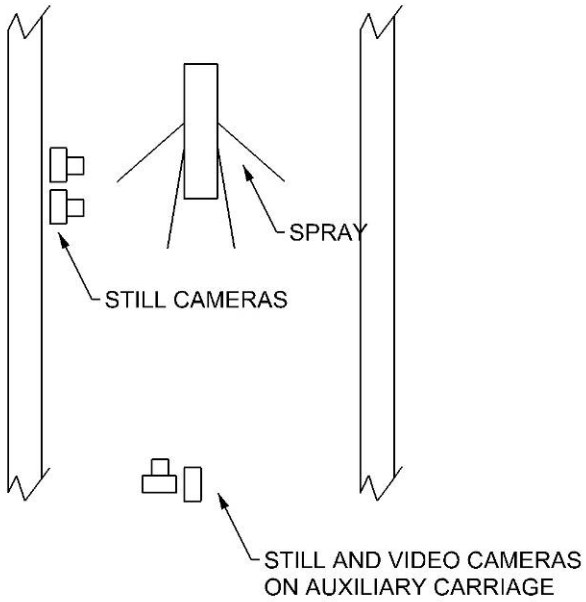

Figure 23: Positions of Cameras used during Spray Tests

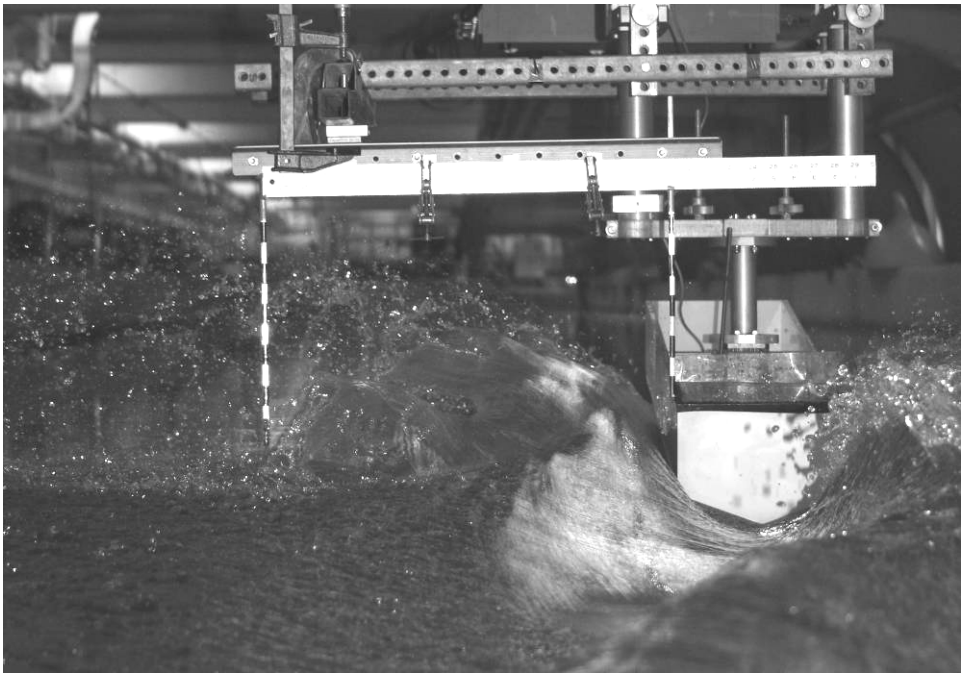

Typical Transverse Photograph

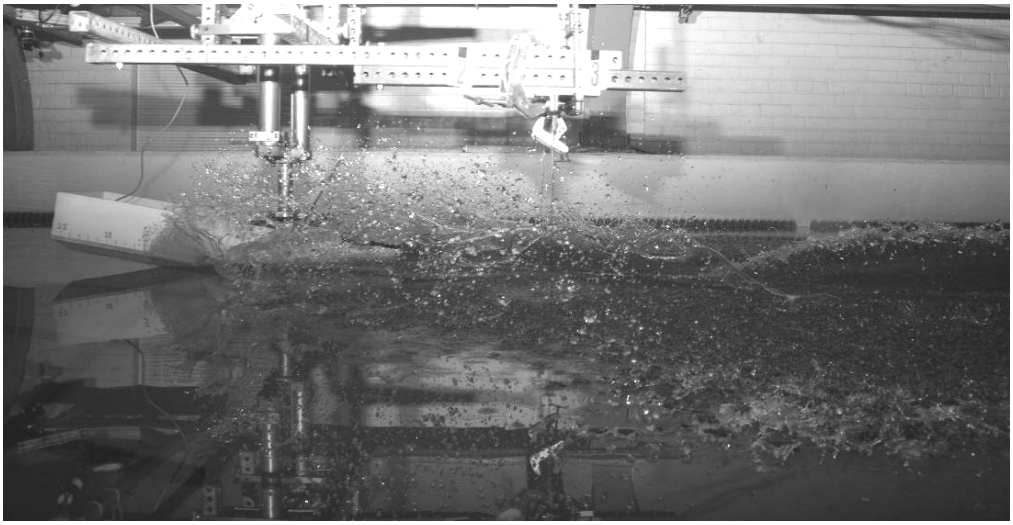

Typical Longitudinal Photograph

Figure 24: Photographs of Model and Reference Grids ($\beta = 20$, $\tau = 8$, Cv = 3)